

MODELING THE EFFECTS OF REGIONAL  
HYDROSTRATIGRAPHY AND TOPOGRAPHY  
ON GROUND-WATER FLOW, PALO DURO BASIN, TEXAS

by

Rainer K. Senger

Graham E. Fogg

Prepared for the  
U.S. Department of Energy  
Office of Nuclear Waste Isolation  
under contract no. DE-AC-97-83WM46615

Bureau of Economic Geology  
W.L. Fisher, Director  
The University of Texas at Austin  
University Station, P.O. Box X  
Austin, Texas 78713

1984

## CONTENTS

ABSTRACT

INTRODUCTION

HYDROGEOLOGY

- Geologic Setting
- Physiography and Climate
- Recharge and Discharge

DATA BASE

- Hydraulic Head and Pressure
- Hydrogeologic Properties
  - Ogallala
  - Dockum
  - Permian Evaporite Strata
  - Lower Permian and Pennsylvanian Strata
  - Salt Dissolution Zones

COMPUTER PROGRAM

MODELING PROCEDURE

- Finite Element Mesh
- Boundary Conditions of the Model
- Simulation Strategy

LIMITATIONS OF THE MODEL

RESULTS AND DISCUSSION

- Granite-wash Permeability
  - Simulation A-1
  - Simulation A-2
  - Simulation A-3
- The Role of the Evaporite Aquitard on Subhydrostatic Conditions
  - Simulation B-1
  - Simulation B-2
- Effect of Pecos River
  - Simulation C
- Hydraulic Interconnection of Ogallala and Dockum Aquifers
  - Simulation D
- Ground-water Flow and Travel Times

SUMMARY AND CONCLUSIONS

REFERENCES

APPENDIX

## ABSTRACT

A cross-sectional ground-water flow model was constructed of the Palo Duro Basin in order to analyze available hydrogeologic data and to better understand causes of the underpressuring below the Evaporite Aquitard and mechanisms of recharge and discharge to and from the Deep-Basin Brine Aquifer. Various effects of lithostratigraphy and topography on subhydrostatic conditions in the deep section were investigated in different simulations.

The model indicates that the subhydrostatic pressures beneath the Evaporite Aquitard are caused by segregation of deep and shallow flow systems by the low permeable evaporite section and drainage of the deep system by relatively permeable granite wash deposits. The Pecos River, which allows underflow of some ground water recharging in the New Mexico area to the west, enhances underpressuring beneath the western half of the High Plains by serving as a discharge area for water that would otherwise move downdip into the Deep-Basin Brine Aquifer. In addition to this recharge, about 26% of the ground water in the Deep-Basin Brine Aquifer originates from leakage through the evaporite section, assuming  $K_z = 2.8 \times 10^{-4}$  md, the upper limit of aquitard permeability suggested by the model.

The ground-water flow pattern within the Deep-Basin Brine Aquifer is governed by the spatial distribution of more permeable strata, in particular, the granite wash deposits. In the cross-sectional model, most of the ground water in the Deep-Basin Brine Aquifer discharges laterally through the eastern boundary and eventually by upward leakage in the easternmost part of the cross section.

Ground-water travel times through the Deep-Basin Brine Aquifer from the westernmost recharge area in New Mexico to the eastern boundary of the model range between 1.2 and 4 million years, depending on the flow path depicted by the stream-tubes and average porosities of the different units.

## INTRODUCTION

Information on the regional hydrogeology of the Palo Duro Basin is important in the investigation of the suitability of this basin for high-level nuclear waste disposal. Predictions of the long-term behavior of a nuclear waste repository require detailed knowledge and understanding of ground-water hydrology in the region surrounding the site. Transportation by ground water is the most likely mechanism by which radionuclides could reach the biosphere from an underground repository.

The Permian Evaporite Aquitard, the general strata for a possible waste site, is underlain by the Deep-Basin Brine Aquifer (Wolfcampian age and older). The Deep-Basin Brine Aquifer is underpressured with respect to water table conditions in the Ogallala and Dockum aquifers overlying the Evaporite Aquitard in the center of the basin. Hydraulic head decreases by as much as 700 m (2,300 ft) from the Ogallala to the bottom of the Evaporite Aquitard. The head difference suggests that (1) permeability of the aquitard is very low and the Ogallala-Dockum aquifer is consequently isolated from the deeper aquifer system, and (2) if contaminants did escape from a repository site within the Evaporite Aquitard, they would move downward rather than upward.

A two-dimensional ground-water flow model was constructed along a cross section through the Palo Duro Basin to investigate causes of the underpressuring below the Evaporite Aquitard and mechanisms of recharge and discharge to and from the Deep-Basin Brine Aquifer. The model simulates steady-state ground-water flow conditions using (1) data on hydraulic conductivity from various hydrologic units in the section and (2) hydraulic head and recharge rates along the boundaries of the model. The scope of the model consists primarily of investigating various factors affecting the overall ground-water flow pattern in the basin, and is not necessarily aimed at achieving the best fit with the observed head data.



## HYDROGEOLOGY

### Geologic Setting

The Palo Duro Basin is a Paleozoic depositional subbasin of the larger Permian Basin of west Texas and southeastern New Mexico. Major structural features such as Bravo Dome, the Amarillo Uplift, and Matador Arch, shown in figure 1 represent the northern and southern boundaries of the Palo Duro Basin (Handford, 1980). The basin extends from the Tucumcari Basin in the west to the Hardeman Basin in the east. The stratigraphy of the basin shows extreme hydrogeologic inhomogeneities which are the result of long-lived cycles of sedimentation in different environments (table 1). Handford and Dutton (1980) distinguish four depositional cycles: (1) formation of the basin and subsequent deposition of basement-derived fan-delta granite wash from uplifts flanking the basin, (2) planation and burial of the uplifts through Early Permian time and infilling of the deep basin with shelf margin carbonate and basinal facies, (3) encroachment of continental red-bed facies from sources in New Mexico and Oklahoma and deposition of thick Middle to Upper Permian marine evaporites in arid environments, and (4) marine retreat during late Permian time and development of a Triassic lacustrine basin brought about as a result of continental rifting and drainage reversal. For detailed information on the tectonostratigraphic setting and depositional environment of the Palo Duro Basin refer to Handford and Dutton (1980) and Dutton and others (1982).

The major hydrogeologic units in the Palo Duro Basin are the Deep-Basin Brine Aquifer of Wolfcampian and Pennsylvanian age and the shallow Ogallala and Dockum aquifers, separated by a thick aquitard of Middle and Upper Permian evaporites (table 1).



## Physiography and Climate

The main topographic features in the Texas Panhandle are the High Plains to the west and the Rolling Plains to the east. The surface of the High Plains is generally smooth and slopes gently eastward at about 2 to 3 m per kilometer (10 to 15 ft per mile) with an elevation ranging from 900 to 1,450 m (3,000 to 4,700 ft) along the cross section (fig. 2). A gentle scarp forms its western limit in eastern New Mexico and the eastern limit is the Caprock Escarpment which has up to 300 m (1,000 ft) of relief. West of the Pecos River, the topography rises toward the Manzano mountain range, reaching an elevation of about 2,130 m (7,000 ft). The Rolling Plains to the east of the Caprock Escarpment are gently eastward dipping plains of low relief developed on relatively nonresistant rocks of Permian age.

The climate of the High Plains region is semiarid. The mean annual precipitation ranges from about 30 cm (12 inches) in the west to 58 cm (23 inches) in the east (Knowles and others, 1982). West of the Pecos River, precipitation generally increases toward the Manzano mountain range to up to 50 cm (20 inches). The mean annual temperature of the High Plains is about 15° C (59° F) with an average difference between summer and winter temperatures on the order of 22° C (40° F).

## Recharge and Discharge

Recharge to the Ogallala aquifer is variable and ranges from 0.145 cm (0.058 inch) to 2.08 cm (0.833 inch) per year, depending on climate, vegetative cover, soil type, and clay or caliche aquicludes at the surface (Knowles and others, 1982). Along the cross section, recharge values assigned to the High Plains of the Texas Panhandle are at a minimum of 0.145 cm (0.058 inch) (Knowles and others, 1982), while in the New Mexico area, recharge rates may be higher due to a sandier soil type. The Pecos River is a major discharge area, primarily for ground water recharging to the

west of the river (Mower and others, 1964). Because of the eastward dipping strata and topography, discharge of ground water from the High Plains to the Pecos is probably small. Most of the ground water in the High Plains aquifer is discharged artificially through wells and naturally through springs and seeps along the Caprock Escarpment. Springs in the Rolling Plains east of the High Plains are characterized by high salinities due to salt dissolution by shallow ground water of Permian evaporite strata east of the Caprock Escarpment (Kreitler and Bassett, 1983; Richter, 1983).

## DATA BASE

### Hydraulic Head and Pressure

Abundant hydraulic head data from the Ogallala aquifer indicate that the shallow ground water generally moves east and southeast under the influence of the regional topographic dip (fig. 3). Although water levels have been declining since 1940 due to heavy pumpage, the regional dip of potentiometric surface of the Ogallala has not changed significantly from pre-pumpage days (Knowles and others, 1982). Even though the heavy pumpage has caused problems for agriculture by a drop in the water table ranging from a few feet to several hundred feet, this change in hydraulic head does not impact the modeling effort.

Hydraulic head data of the Deep-Basin Brine Aquifer were derived from results of drill-stem tests, which were converted into fresh-water heads. An evaluation of pressure data is given in Wirojanagud and others (1984), who constructed a hydraulic head map for the Deep-Basin Brine Aquifer (fig. 4). A comparison of unconfined and confined hydraulic heads shows that heads in the Deep-Basin Brine Aquifer are lower than heads in the Upper Aquifer (fig. 5). The head difference generally decreases toward the south and to the east of the Caprock Escarpment where land surface rapidly drops in elevation by about 330 m (1,000 ft).

## Hydrogeologic Properties

### Ogallala Formation

The Ogallala Formation consists primarily of fluvial clastics which were deposited over an irregular Triassic surface in a deltaic system of overlapping fan lobes (Seni, 1980). The percentage of sand and gravel generally decreases from west to east across the High Plains. Average hydraulic conductivity of the Ogallala is 8.0 m/day based on pumping test results reported in Myers (1969). Vertical permeability was assumed to be one order of magnitude less than horizontal permeability, due to horizontal stratification of sands and muds in the formation.

### Dockum Group

The Dockum Group represents a fluvial and lacustrine depositional system, which is composed of interrelated clastic facies containing regionally extensive lacustrine mudstones. Percentage of sand within the Dockum varies between 40 percent and 10 percent (McGowen and others, 1979). Average hydraulic conductivity for the Dockum sands is about 0.8 m/day based on pumping test results (Myers, 1969).

Most modeling approaches (INTERA, 1983; Wirojanagud and others, 1984) assume that the potentiometric surface of the Ogallala is representative of the Dockum as well. There is evidence, however, that hydraulic heads in the Dockum are significantly lower (30 to 90 m, 100 to 300 ft) than those in the Ogallala (Fink, 1963; Stevens, unpublished data). Also, the water chemistry and the  $O^{18}$  and  $H^2$  concentration of ground water in the Dockum is different from that in the overlying Ogallala aquifer (Seni, 1977; Senger and others, in preparation), suggesting that the two aquifers are generally not well interconnected.

The Dockum is a sand-poor unit containing regionally extensive lacustrine mudstones. Vertical permeability of the Dockum is, therefore, probably very low. As shown in simulation D of this study, vertical permeability has to be at least four orders



of magnitude lower than horizontal permeability in order for the model to simulate a significant head difference of up to 30 m (100 ft) between the Ogallala and Dockum aquifers.

#### Permian Evaporite Strata

The Permian evaporite strata include deposits of evaporites, and of inner shelf systems (fig. 2). The Evaporite Aquitard in the Palo Duro Basin consists mainly of thick layers of salt deposits, anhydrite, red beds, and peritidal dolomite (McGowen, 1981). A vertical permeability of 0.00028 md for the Evaporite Aquitard was derived from the harmonic means of permeabilities using typical and measured values of permeability for each sub-strata (Wirojanagud and others, 1984). The permeability value is at best a rough estimate and does not incorporate possible effects of fractures which could increase vertical leakage through the evaporite section.

#### Lower Permian and Pennsylvanian Strata

Lower Permian, Pennsylvanian, and Pre-Pennsylvanian formations constitute the Deep-Basin Brine Aquifer (table 1). The depositional environments during Lower Permian (Wolfcampian) and the Pennsylvanian were similar and consisted of (fig. 2) (1) fan-delta system, (2) shelf and shelf-margin systems, and (3) a basinal system (Handford and Dutton, 1980; Dutton and others, 1982). The fan-delta system is composed of arkosic sands and conglomerates (granite wash) which were derived from the igneous and metamorphic uplifts surrounding the Palo Duro Basin. Open marine shelf carbonates and terrigenous muds comprise the shelf and basinal system. The top of the Wolfcamp is marked by a basinwide distribution of shelf-margin facies (Brown Dolomite) that resulted from a southward shift of the shelf break which terminated deposition of basinal facies in the area (Handford, 1980).

Wirojanagud and others (1984) combined permeability data based on limited analyses of drill stem tests, pumping tests, and compiled data by Core Lab, Inc. (1972)

and derived average permeabilities and variances of the different hydrologic units within the Deep-Basin Brine Aquifer (table 2). For comparison, average permeability values and variances for the different types of tests were compiled by Smith (1983).

Vertical permeabilities for the Lower Permian and Pennsylvanian strata are generally assumed to be two orders of magnitude lower than horizontal permeability due to the horizontal stratification within each hydrologic unit. Values of permeability were converted to hydraulic conductivity using an average fluid salinity and temperature of 127,000 mg/L and 46° C (115° F), based on data from Bassett and Bentley (1982). For these fluid properties 1 md equals 0.00115 m/day.

The permeability data from the Deep-Basin Brine Aquifer show large variances (log-normal) of up to 7.13 suggesting an extremely heterogeneous distribution of permeabilities and a relatively small data base (table 2). Proximal granite-wash deposits closer to the source areas (Amarillo Uplift, Bravo Dome, and Wichita Mountains) apparently have higher permeabilities than distal granite-wash deposits in the center of the basin. Five pumping tests from proximal granite wash in the J. Friemel #1 well located in northeastern Deaf Smith County yielded permeabilities of 10 md to 400 md with an average of 140 md, which is much higher than the geometric mean of 8.6 md. Relatively high permeabilities of 250 md in proximal granite wash were also suggested by Wirojanagud and others (1984).

Measured permeability data for the Permian/Pennsylvanian strata labeled "mud-flat and alluvial fan delta systems" on the left side of figure 2 were not available. Therefore, a generic value of permeability of about 70 md (equivalent to a hydraulic conductivity of  $8.2 \times 10^{-2}$  m/day) as suggested by Bassett and others (1981) was assigned to the westernmost hydrologic unit based on typical values for comparable geologic materials (Freeze and Cherry, 1979). Using this typical permeability value, the model computed a discharge rate to the Pecos River of about 1.3 m<sup>3</sup>/day, which is

in agreement with reported data on rate of streamflow increase along the Pecos River in this area (Mower and others, 1964).

### Salt Dissolution Zones

Permeabilities for the units representing the salt dissolution zones located east and west of the High Plains in figure 2 were conservatively estimated to be 70 md (equivalent to 0.082 m/day), that is much higher than the permeability of the adjacent aquitard (fig. 3) due to intense faulting and collapse of the formation overlying the salt deposits. Recent hydrologic testing in the DOE salt dissolution wells yielded relatively high hydraulic conductivities of about 0.17 m/day (Dutton, in preparation). The eastward extension of the Permian salt strata is represented by a mudflat system (fig. 3) with permeabilities derived from generic values as suggested by Bassett and others (1981).

### COMPUTER PROGRAM

The model was implemented with the computer program FREESURF, developed by Neuman and Witherspoon (1970). FREESURF was used to solve the partial differential equation describing two-dimensional steady-state ground-water flow in porous media:

$$\frac{\partial}{\partial x} (K_x \frac{\partial h}{\partial x}) + \frac{\partial}{\partial z} (K_z \frac{\partial h}{\partial z}) = 0$$

where  $K_x$  and  $K_z$  are horizontal and vertical hydraulic conductivity, respectively. FREESURF uses a finite element method and a direct solution technique (Gaussian elimination). Full descriptions of the program and its capabilities are available in the User's Guide for FREESURF I (Neuman, 1976). Examples of application and its performance are documented according to QA guidelines in Fogg and Senger (1983).

The program computes hydraulic heads at each node and fluxes along prescribed head boundaries representing recharge or discharge. In addition, the program was used

to compute the stream functions at each node based on the results of the steady-state hydraulic heads and fluxes along the inflow and outflow boundaries. The computed streamlines show ground-water flow patterns and fluxes which are difficult, if not impossible, to discern from the contour maps of computed hydraulic heads, owing to anisotropic hydraulic conductivity values and extreme vertical exaggeration of the cross-sectional model. For details concerning the computation of streamlines, refer to Fogg and Senger (in preparation).

## MODELING PROCEDURE

### Finite Element Mesh

The ground-water flow model was constructed along an east-west cross section extending from New Mexico across the Texas Panhandle into Oklahoma (fig. 2). The finite element mesh was designed to represent the geometry of the different depositional facies (fig. 6). Due to extreme vertical exaggeration, the large node spacing differences between horizontal and vertical directions could cause numerical errors in the solution. In Appendix A, the effect of extreme vertical exaggeration was tested by successively decreasing the node spacing in vertical direction of a simple rectangular mesh. Figure A2 shows that the errors in computed hydraulic head are small and can be considered negligible for most practical purposes.

In figure 6, three hydrologic units are distinguished within the Deep-Basin Brine Aquifer, based on the lithostratigraphy: (1) carbonate shelf and shelf-margin systems, (2) mud-filled basin and slope system, and (3) fan delta system (granite wash). The Permian evaporite sequence is represented as a thick aquitard separating the Deep-Basin Brine Aquifer from the overlying Ogallala and Dockum fresh-water aquifers. Additional hydrogeologic units represented in the model are the salt dissolution zones to the east and to the west of the High Plains, a Permian mudflat system extending



into Oklahoma, and the Permian/Pennsylvanian mudflat and alluvial fan delta systems in New Mexico.

#### Boundary Conditions of the Model

In the model, two types of boundary conditions are applied: (1) prescribed heads (Dirichlet boundary condition) and (2) prescribed flux (Neumann boundary condition). The upper surface of the finite element mesh corresponds approximately to the water table and generally follows the topography (water-level declines caused by ground-water pumpage are ignored in the model). To the east and west of the High Plains, the water table is represented with prescribed head boundary conditions. Information on the amount of recharge to the Ogallala aquifer along the High Plains (Knowles and others, 1982) permitted assignment of prescribed fluxes at the corresponding boundary nodes. A recharge value of 0.145 cm (0.058 inch) was assigned along the High Plains in the Texas Panhandle and increased to 0.625 cm (0.250 inch) to account for the sandier soil type in the New Mexico area. The prescribed flux boundary condition along the High Plains surface, however, required a reduction of hydraulic conductivities by one order of magnitude in both the Ogallala and Dockum aquifers in the western High Plains in New Mexico in order for the model to produce the observed water levels of the Ogallala aquifer with reasonable accuracy (fig. 6). This reduction in hydraulic conductivity does not necessarily represent a calibration of "true" aquifer properties based on the available hydraulic head data but may reflect the discrepancy in vertical geometry between the actual northwest to southeast flow direction of the High Plains aquifer and the imposed west-east flow direction in the cross-sectional model.

The lower boundary of the mesh was assumed to be impervious and corresponds to the contact between the Deep-Basin Brine Aquifer and basement rocks. Head was assumed to be uniform with depth on the eastern boundary, implying horizontal flow at this boundary. Pressure-depth data from Jackson County, Oklahoma which is located

approximately at the eastern edge of the cross section show a slope of the pressure-depth regression line equivalent to brine-hydrostatic (fig. 7).

### Simulation Strategy

Different numerical simulations were run for the cross-sectional model (table 3). The results are compared to the hydraulic heads derived from the kriged head map of the Deep-Basin Brine Aquifer (fig. 4). The purpose of the simulations was not necessarily aimed at achieving the best fit with the observed head data. The primary objective was to investigate the importance of various factors affecting the overall ground-water flow pattern in the basin.

Simulations A-1 and A-2 test possible spatial permeability variations of granite-wash deposits. While in Simulation A-1 a uniform permeability distribution for granite wash is used throughout the basin ( $K=8.6$  md), in Simulation A-2 proximal granite wash deposits in the eastern part of the cross section are assigned a permeability value of 100 md, which is about 10 times higher than the geometric mean in table 2. Simulation A-3 incorporates the possible draining effect of proximal granite-wash deposits along the Oldham Nose and Amarillo Uplift north of the cross-sectional traverse by inserting artificially high values of granite-wash permeability throughout the entire east-west cross section. Although computed heads in Simulation A-3 agree better with kriged heads in the deep section, Simulation A-2 is considered the most realistic model supported by the permeability data which are presently available for the Deep-Basin Brine Aquifer.

Simulations B-1 and B-2 investigate the effect of leakage through the Evaporite Aquitard by varying vertical permeability of the aquitard ( $2.8 \times 10^{-3}$  to  $2.8 \times 10^{-7}$  md). The model is used to give a possible range of permeabilities for the aquitard and to test the validity of the assumed permeability value listed in table 2.

In Simulation C, the effect of the Pecos River on the subhydrostatic conditions in the Deep-Basin Brine Aquifer is tested. For this purpose, the finite element mesh is modified to eliminate the topography of the Pecos River valley by extending the general slope of the High Plains surface toward the mountain range at the western boundary of the cross section (fig. 14).

The hydraulic interconnection between the Ogallala and the Dockum was addressed in Simulation D. By reducing vertical permeability of the Dockum in successive runs, the observed hydraulic head differential in the shallow aquifer system was modeled and its effect on leakage rate through the Evaporite Aquitard, and on heads in the deep section, is investigated.

#### LIMITATIONS OF THE MODEL

When comparing the results of the model with observed data, it is important to recognize that the regional ground-water flow direction in the Wolfcamp Aquifer is toward the northeast (Wirojanagud and others, 1984), while the potentiometric surface representative for the whole Deep-Basin Brine Aquifer (fig. 4) shows a more west to east flow component. Thus, results of the model, which simulates ground-water flow along an east-west transverse across the Palo Duro Basin, are not always directly comparable to field conditions.

Major potential sources of errors in the model are the hydraulic conductivities and assumed anisotropies of the different hydrologic units. With the exception of the granite wash, which was subdivided into distal and proximal deposits, uniform permeabilities were assigned to the hydrologic units in the deep section ignoring possible lateral and vertical permeability trends throughout the basin. Large values of variance of measured permeabilities (table 2) suggest large natural variations in permeabilities of the hydrologic units. The data are, however, insufficient to map spatial permeability distributions within the different units. For some units where

measured permeability values were not available (i.e., Evaporite Aquitard, Permian/Pennsylvanian mudflat and alluvial/fan delta system), assumed permeability values had to be used based on typical values for the geologic material (Freeze and Cherry, 1979).

Discretization of the cross-sectional model required simplification and conceptualization of the lithostratigraphy of the basin. Ground-water flow pattern on a local scale could therefore be much more complex than those depicted by the model.

An assumption of the ground-water flow model is the existence of steady-state flow conditions. Bassett and Bentley (1983) indicated that the Deep-Basin Brine Aquifer may have been a through-flowing aquifer system since the early Tertiary. However, it is possible that present conditions may be transient and that pressures at depth are still adjusting to the hydraulic-head conditions imposed by the more recent Ogallala aquifer (Bassett and Bentley, 1983). Other phenomena that might cause transient conditions of the hydrodynamics of the Palo Duro Basin include: (1) uplift and tilting of the basin might have caused an increase of hydraulic potentials along the western surface relative to the surface potentials in the east; (2) erosion and retreat of the Caprock Escarpment could result in topographic effects on the hydrology, and in dilation of the underlying units causing a gradual change in aquifer properties; and (3) extensive hydrocarbon production in the Panhandle Gas and Oil field causing a general decline in reservoir pressures could affect the hydrostatic pressures in the Deep-Basin Brine Aquifer.

Another limitation of the model is the assumption of a homogeneous fluid throughout the basin; that is, density and temperature effects were omitted in the model. Assuming increased salinities with depth, the increase in fluid density leads to greater gravitational forces, and to an increase in viscosity. Increased viscosity results in a decrease of hydraulic conductivity and influences flow rates in a linear



fashion. Future modeling efforts are planned which incorporate density variations and investigate its effects on fluid potentials.

## RESULTS AND DISCUSSION

### Granite-Wash Permeability

#### Simulation A-1

In Simulation A-1, permeabilities of the different hydrologic units were assigned according to table 4. The permeability value for the shelf carbonate in the Deep-Basin Brine Aquifer is a weighted arithmetic average of permeabilities represented by the geometric means of the different stratigraphic units in table 2: Wolfcampian carbonate, Pennsylvanian carbonate, and Pre-Pennsylvanian rocks.

Hydraulic heads computed by the model in Simulation 1 indicate two different flow regimes (fig. 8): (1) a shallow flow system governed primarily by topography, and (2) a deeper flow regime recharging in the New Mexico area and passing deep beneath the Pecos River, which acts as a ground-water flow divide in the upper part of the cross section. The thick evaporite section in the center of the cross section effectively isolates the two flow systems.

Beneath the High Plains, hydraulic heads computed by the model in the Deep-Basin Brine Aquifer are up to 300 m (1000 ft) lower than hydraulic heads in the Ogallala (fig. 8). East of the Caprock Escarpment, heads in the deep section become progressively higher by up to 75 m (246 ft) than heads in the unconfined section which represents unrealistic conditions. A comparison of kriged heads in the Deep-Basin Brine Aquifer (fig. 4) and observed heads in the unconfined aquifers (fig. 3) indicates that beneath the evaporite section in the center of the basin hydraulic heads are lower by more than 400 m (1312 ft) than those in the Ogallala and hydraulic heads east of the Caprock Escarpment do not exceed land surface elevation. Only toward the Texas-

Oklahoma border do kriged heads in the deep section approach hydrostatic conditions. In Simulation A-2, we attempted to correct these discrepancies.

#### Simulation A-2

As mentioned earlier, higher permeability values are more likely in proximal granite-wash deposits in the eastern part of the cross section than in distal granite wash in the center of the basin owing to a presumed decrease in grain size away from the source area. In Simulation A-2, a permeability value of 100 md was assigned to granite wash east of the Caprock Escarpment in the proximal facies. As a result, computed hydraulic heads in the Deep-Basin Brine Aquifer east of the escarpment no longer exceed heads in the shallow interval (fig. 9).

In general, the computed heads in the eastern half of the cross section show good agreement with kriged head data in the Deep-Basin Brine Aquifer. The resulting decrease of hydraulic heads in the eastern part compared to heads in Simulation A-1 demonstrates the importance of the relatively permeable granite-wash deposits. The granite wash effectively drains the deeper section with greater ease than it can be recharged. The evaporite section effectively isolates the deeper aquifers from the higher hydraulic heads of the Ogallala and Dockum aquifers, as will be demonstrated later.

In the western half of the cross section computed heads in the deep section become progressively higher by up to 300 m (1000 ft) than kriged heads in both Simulations A-1 and A-2. Because of the distance of about 150 km (93 miles) from the Texas-New Mexico border to the Caprock Escarpment in the east, the draining effect of the relatively permeable granite-wash deposits in the east does not influence the western part of the Deep-Basin Brine Aquifer. The discrepancy in hydraulic heads could be an artifact of the geometry and the direction of the cross-sectional model.

Wirojanagud and others (1984) show that relatively permeable granite-wash deposits along the Amarillo Uplift and Bravo Dome are important factors controlling the regional ground-water flow direction in the Deep-Basin Brine Aquifer. Proximal granite wash occurring to the north of the cross section (fig. 10) was found to have good permeability as indicated by pumping test results in the J. Friemel #1 well located in northeastern Deaf Smith County. The possible draining effect of these deposits, however, is not considered in the east-west cross-sectional model which could explain the discrepancy between computed hydraulic heads and the kriged heads in the western part of the Deep-Basin Brine Aquifer.

The computed streamlines in figure 11 correspond to the head solution in Simulation A-2 (fig. 9). The region defined by two adjacent streamlines contains a constant volumetric flow rate. The streamline distribution shows that ground-water flow is concentrated in the shallow aquifer system. Each streamtube in the shallow section (shaded pattern) carries  $0.2 \text{ m}^3/\text{d}$  while each streamtube in the deeper section carries only  $0.01 \text{ m}^3/\text{d}$ . Only  $0.044 \text{ m}^3/\text{d}$ , or about 0.1 percent of the total ground-water inflow of  $4.34 \text{ m}^3/\text{d}$ , passes through the Deep-Basin Brine Aquifer (fig. 11).

The streamline distribution in figure 11 shows that ground water within the Deep-Basin Brine Aquifer is flowing down the structural dip into the central basin. East of the central basin ground-water flow is concentrated in the more permeable granite-wash deposits and discharge occurs laterally through the eastern boundary.

#### Simulation A-3

The purpose of this simulation is to consider possible draining effects of proximal granite wash to the northeast of the cross section along the Amarillo Uplift and Oldham Nose, by inserting artificially high values of granite-wash permeability along the entire east-west cross section. In addition, information on the occurrence of thick granite-wash deposits in northeastern New Mexico (SWEC, 1983) was incorporated in

the model by extending the Permian-Pennsylvanian fan-delta system into New Mexico. Granite-wash permeability was increased from 8.6 md to 100 md for distal facies to the west and from 100 md to 250 md for proximal granite wash to the east of the Caprock Escarpment. As mentioned earlier, pumping-test results in J. Friemel #1 well indicated permeability values of up to 400 md for proximal granite wash.

The computed hydraulic heads (fig. 12) in the Deep-Basin Brine Aquifer are significantly lower in the western part of the cross section compared to the previous Simulation A-2. Overall, heads in the deep section agree reasonably well with kriged heads in figure 4. The corresponding streamlines in figure 13 show that the amount of ground-water flow through the Deep-Basin Brine Aquifer increased from 0.044 in Simulation A-2 to 0.081 m<sup>3</sup>/day and flow follows predominantly the permeable granite wash deposits. Leakage through the Evaporite Aquitard increased from 0.0094 in Simulation A-2 to 0.0116 m<sup>3</sup>/day in this simulation due to the increased hydraulic gradient across the Evaporite Aquitard. A possible increase in permeability of the porous carbonates (Handford and Dutton, 1980; Herron, personal communication, 1984), which was considered in the planar ground-water flow model in Wirojanagud and others (1984) does not significantly change hydraulic heads and the overall ground-water flow pattern in the deep section in the cross-sectional model. The resulting decrease of hydraulic heads in the western part of the Deep-Basin Brine Aquifer in Simulation A-3 compared to Simulation A-2 indicates the importance of the granite-wash deposits acting as a hydrologic sink.

The general ground-water flow pattern indicates two important aspects regarding the hydrology of the Palo Duro Basin: (1) role of the Evaporite Aquitard in isolating the deeper aquifers from the higher hydraulic heads of the Ogallala and Dockum aquifers; and (2) discharge to the Pecos River. The river serves as major discharge point of ground water recharging in the west that would otherwise flow into the Deep-Basin Brine Aquifer. Therefore, one possible reason for underpressuring in



the deep section to the east could be insufficient recharge to the Deep-Basin Brine Aquifer due to the deflection of ground-water flow upward to the Pecos River.

#### Role of the Evaporite Aquitard on Subhydrostatic Conditions

The Evaporite Aquitard is thought to be an important cause of the subhydrostatic conditions in the deep aquifer because it isolates the deep basin system from the higher hydraulic heads in the High Plains aquifer. In other words, if the Evaporite Aquitard were absent, the Deep-Basin Brine Aquifer and the Ogallala would be hydraulically connected and their heads would be similar. In Simulations B-1 and B-2, this hypothesis is tested by first increasing and second by decreasing aquitard permeability. Also, by investigating the effects of varying aquitard permeabilities on the head distribution in the deep section, a range of possible aquitard permeabilities is obtained.

##### Simulation B-1

Increasing aquitard permeability from  $2.8 \times 10^{-4}$  md (Simulation A-2) to  $2.8 \times 10^{-3}$  md in Simulation B-1 results in a significant increase in hydraulic heads of up to 250 m in the deep section (fig. 14). The computed heads became unrealistically high which suggests that the generically-derived permeability value of  $2.8 \times 10^{-4}$  md (Simulation A) represents an upper limit of possible permeability values for the Evaporite Aquitard. In comparison, Wirojanagud and others (1984) inferred a permeability value of  $8 \times 10^{-5}$  md from their "best" simulation of a horizontal-plane ground-water flow model. They concluded that leakage through the Evaporite Aquitard is significant and accounts for about 30 percent of the total flow through the Deep-Basin Brine Aquifer.

## Simulation B-2

In Simulation B-2, the aquitard permeability was decreased by 5 orders of magnitude from  $2.8 \times 10^{-4}$  md to  $2.8 \times 10^{-9}$  md. The results in figure 15 show a general decrease of hydraulic heads in the Deep-Basin Brine Aquifer by up to 50 m in the central part of the cross section compared to results of Simulation A-2, and slightly lower heads than kriged heads in the eastern part of the cross section.

In the western part of the deep section, changes in computed heads were much smaller, indicating that a drastic decrease of leakage through the Evaporite Aquitard (less than  $10^{-7}$  m<sup>3</sup>/day) does not significantly reduce computed hydraulic heads in eastern New Mexico.

## The Effect of the Pecos River

In order to evaluate the effect of the Pecos River on subhydrostatic conditions in the Palo Duro Basin, the finite element mesh was modified in Simulation C such that the general slope of the High Plains topography extended to the Manzano mountain range in New Mexico, eliminating the Pecos River valley. Recharge rates to the Ogallala at the prescribed flux boundaries had to be artificially reduced in order to simulate the observed water level on the High Plains. In addition to recharge along the High Plains, ground water recharging west of the Pecos River flows into the Ogallala and Dockum aquifers, which would increase the hydraulic heads in the High Plains aquifer.

## Simulation C

Computed heads in figure 16 increase in the western part of the Deep-Basin Brine Aquifer relative to computed heads in Simulation A-2 (fig. 9). Heads in the eastern part, however, do not change significantly and still display subhydrostatic conditions. Ground-water flow into the Deep-Basin Brine Aquifer, west of the Pecos

River, increases from 0.034 m<sup>3</sup>/day in Simulation A-2 to 0.047 m<sup>3</sup>/day in this simulation (fig. 17). The streamline distribution indicates that most of the flow lines are still deflected upward to the surface at the facies contrast between the Permian-Pennsylvanian mudflat and fan-delta system to the west and the Evaporite Aquitard in the center of the cross section. Hence, the facies contrast rather than topography is the more important cause of upward flow of ground water beneath the Pecos Valley.

The increase in ground-water recharge to the deep section in Simulation C affects hydraulic heads in the western half of the cross section. However, heads in the eastern part did not change significantly, indicating that the topographic effect of the Pecos River on the hydrologic regime is restricted to the updip section of the Deep-Basin Brine Aquifer. Ground-water discharge to the Pecos does not significantly affect subhydrostatic conditions in the eastern part of the cross section.

The effect of the Pecos River on hydraulic heads in the deep section would probably increase if the relatively permeable granite-wash deposits extended far into the New Mexico area, which could result in an increase of ground-water flow from the west into the Deep-Basin Brine Aquifer. However, our geologic data indicate that granite-wash deposits are pinching out east of the Pecos (Handford and others, 1981). Furthermore, head maps from the Deep-Basin Brine Aquifer (Smith, in preparation; SWEC, 1983) show steep hydraulic gradients in eastern New Mexico which suggest a zone of low permeability in the deep section. This would restrict possible underflow beneath the Pecos River of recharge water from the western outcrop area.

#### Interconnection of Ogallala and Dockum Aquifers

In the previous simulations, the Ogallala and Dockum aquifers were well-interconnected inasmuch as vertical flow between the two aquifers was not restricted by low values of hydraulic conductivity. Accordingly, heads did not differ appreciably between the two aquifers. However, Fink (1963) and Stevens (unpublished data)

indicate that at places, hydraulic heads in the Santa Rosa member of the Dockum are about 30 to 100 m (100 to 300 ft) lower than heads in the Ogallala. In order to model a significant hydraulic head difference across the shallow aquifer system, vertical hydraulic conductivity of the Dockum was lowered in successive runs of the model until the minimum observed head difference was simulated in the model.

A significant head difference between the Ogallala and the Dockum results in reduced hydraulic gradients across the evaporite section, which in turn affects the amount of leakage through the Evaporite Aquitard.

#### Simulation D

Using  $K_z = 8 \times 10^{-2}$  m/day for the Ogallala and  $K_z = 8 \times 10^{-5}$  m/day for the Dockum (2 and 4 orders of magnitude lower than  $K_x$ , respectively), computed heads in the Dockum were lower than in Simulation A-2 by up to 40 m (130 ft) as shown in figure 18. The head difference of 40 m between the Ogallala and the Dockum, however, is not continuous throughout the section but represents the maximum head difference in the western part of the shallow aquifer system (fig. 18).

The change in vertical hydraulic gradient in the shallow aquifer system results in slightly lower heads in the deep section (less than 4 m or 13 ft) than those in Simulation A-2. The resulting decrease of up to 35 m (115 ft) in the hydraulic head difference across the Evaporite Aquitard, compared to that in Simulation A-2, reflects the decrease in heads at the base of the Dockum due to reduced flow between the Ogallala and Dockum. The general ground-water flow pattern in the deep section as shown by the computed streamlines (fig. 19) does not change noticeably. However, leakage through the evaporites beneath the High Plains decreased from  $0.0094 \text{ m}^3/\text{day}$  to  $0.0075 \text{ m}^3/\text{day}$ , which is a 19 percent reduction in leakage rate from that in Simulation A-2. Vertical hydraulic gradients in the shallow aquifer systems and their effect on leakage through the Evaporite Aquitard could be important.

The head drop between the Ogallala and the Dockum computed by the model is a conservative value, considering the range of observed head differences of 30 to 120 m (100 to 400 ft) (Fink, 1963). A steeper, vertical gradient between the Ogallala and Dockum aquifers will significantly reduce leakage through the Evaporite Aquitard. This vertical gradient can be increased by further decreasing vertical permeabilities in the shallow aquifer system. It can be shown that, using  $K_x/K_z = 10^5$ , which is only one order of magnitude higher than  $K_x/K_z$  in this simulation, computed heads at the base of the Dockum would be lower by up to 150 m (490 ft) than heads in the Ogallala, and computed leakage through the Evaporite Aquitard would reduce from 0.0075 m<sup>3</sup>/day to 0.0045 m<sup>3</sup>/day.

#### Ground-water Flow Rates and Travel Times

Despite the better agreement between computed heads and kriged heads in Simulation A-3, Simulation A-2 represents the most realistic model which incorporates permeability values for granite wash deposits supported by the presently available data on permeability for the Deep-Basin Brine Aquifer (table 2).

Specific discharge rates of ground-water flow may be obtained by dividing the flow rate represented by a streamtube by its width. In addition, pore-fluid velocity is given by dividing specific discharge by porosity. In Simulation A-2 (fig. 11) the model gives values of specific discharge for the shallow section in the range of  $3 \times 10^{-4}$  to  $2 \times 10^{-2}$  m/day and for the deep section of  $8 \times 10^{-6}$  to  $10^{-4}$  m/day. Maximum ground-water flow velocity in the Ogallala aquifer is about  $1.5 \times 10^{-1}$  m/day, assuming a porosity of 16 percent (Knowles and others, 1982). In the Deep-Basin Brine Aquifer the model indicates maximum ground-water flow velocities in the shelf carbonates of  $1.1 \times 10^{-4}$  m/day and in the proximal granite wash of  $4.4 \times 10^{-4}$  m/day (equivalent to about 400 m and 1,600 m per 10,000 years). Average porosities are assumed to be 8 and 23 percent, respectively, according to Wirojanagud and others (1984).



These flow rates are only rough estimates, and more accurate values will depend on acquisition of new, more detailed data on porosity and permeability distribution in the deep section, and on the construction of improved models.

Leakage rate through the evaporite section is only about  $6 \times 10^{-8}$  m/day. Nevertheless, because of its vast area, the evaporite section beneath the High Plains contributes by vertical leakage about  $0.0094 \text{ m}^3/\text{day}$  to the deep aquifer or 26 percent of the water passing through the Deep-Basin Brine Aquifer, according to the model. The accuracy of this rate is dependent on accuracy of vertical permeability of the aquitard and the head drop across it. In Simulation A-3, computed hydraulic heads in the western part of the deep section are significantly lower than heads in Simulation A-2. The increase in head drop across the aquitard results in an increase in vertical leakage from  $0.0094 \text{ m}^3/\text{day}$  to  $0.0116 \text{ m}^3/\text{day}$  in Simulation A-3.

Ground-water travel times through the Deep-Basin Brine Aquifer from the westernmost recharge area in New Mexico to the eastern boundary of the model (Simulation A-2) range between 1.2 and 4 million years depending on the flow path depicted by the streamtube and average porosities of the different units.

## SUMMARY AND CONCLUSIONS

The observed underpressuring in the Deep-Basin Brine Aquifer can be explained by relatively permeable granite-wash deposits within the Lower Permian/Pennsylvanian strata and the thick, low-permeability Evaporite Aquitard in the center of the basin. The granite wash effectively drains the deeper section more easily than it can be recharged, and the evaporite sequence effectively isolates the deeper section from the shallow Ogallala and Dockum aquifers above the evaporite section. The ground-water flow model also indicates that the Pecos River acts as a ground-water flow divide only in the upper section, and allows underflow of some ground water recharging in the New Mexico area to the west (Summers, 1981). The Pecos River apparently

enhances the underpressuring beneath the western half of the High Plains by serving as a discharge area for some of the ground water that would otherwise move downdip into the Deep-Basin Brine Aquifer. In the eastern half of the cross section, the effect of relatively permeable granite wash acting as a hydrologic sink is probably the dominant factor controlling subhydrostatic conditions.

A significant head difference between the Ogallala and Dockum aquifers can affect the amount of leakage through the Evaporite Aquitard without significantly changing heads in the Deep-Basin Brine Aquifer. Therefore, detailed information on the vertical hydraulic gradient in the units overlying the salt section is needed to establish the specified head boundary and the amount of leakage through the evaporite section. In addition to leakage through the Evaporite Aquitard, ground water in the Deep-Basin Brine Aquifer originates primarily in the New Mexico area and flows beneath the Pecos River into the central basin. The model indicates that the ground-water flow pattern within the Deep-Basin Brine Aquifer is governed by the spatial distribution of more permeable strata, in particular, the granite-wash deposits. The hydraulic head distributions and the general ground-water flow pattern generated in the model agree reasonably well with observed heads and pressure-depth interpretations (Orr, 1984).

## REFERENCES

- Bassett, R. L., and Bentley, M. E., 1982, Geochemistry and hydrodynamics of the deep formation brines in the Palo Duro and Dalhart basins, Texas, USA: *J. Hydrol.*, v. 59, p. 331-372.
- Bassett, R. L., Bentley, M. E., and Simpkins, W. W., 1981, Regional ground-water flow in the Panhandle of Texas: a conceptual model, in Gustavson, T. C., and others, *Geology and geohydrology of the Palo Duro Basin, Texas Panhandle: The University of Texas at Austin, Bureau of Economic Geology Geological Circular 81-3.*
- Core Laboratories, Inc., 1972, A survey of the subsurface saline water of Texas, vol. 3, *Aquifer rock properties: Texas Water Development Board, Report 157, 364 p.*
- Davis, S. N., 1980, Hydrogeologic effects of natural disruptive events on nuclear waste repositories: *Research Report No. PNL-2858, Pacific Northwest Lab., 33 p.*
- Davis, S. N., and DeWiest, R. J., 1966, *Hydrogeology: John Wiley & Sons, New York, 463 p.*
- Dutton, A. R., in preparation, Hydrogeologic testing in the salt dissolution zone of the Palo Duro basin, Texas Panhandle, The University of Texas at Austin, Bureau of Economic Geology, Geological Circular.
- Dutton, S. P., Finley, R. J., Galloway, W. E., Gustavson, T. C., Handford, C. R., and Presley, M. W., 1979, *Geology and geohydrology of the Palo Duro Basin, Texas*

Panhandle; a report on the progress of nuclear waste isolation feasibility studies (1978): The University of Texas at Austin, Bureau of Economic Geology Geological Circular 79-1, 99 p.

Dutton, S. P., Goldstein, A. G., and Ruppel, S. C., 1982, Petroleum potential of the Palo Duro Basin, Texas Panhandle: The University of Texas at Austin, Bureau of Economic Geology Report of Investigations No. 123, 87 p.

Fink, B. E., 1963, Ground-water geology of Triassic deposits, northern part of the Southern High Plains of Texas: High Plains Underground Water Conservation District No. 1, Report No. 163, 79 p.

Fisher, R. S., and Kreitler, C. W., in preparation, Hydrochemistry of Palo Duro brines, in Gustavson, T. C., and others, Geology and geohydrology of the Palo Duro Basin, Texas Panhandle: The University of Texas at Austin, Bureau of Economic Geology Geological Circular.

Fogg, G. E., and Senger, R. K., 1983, QA documentation of the program FREESURF: The University of Texas at Austin, Bureau of Economic Geology, QA document.

Fogg, G. E., and Senger, R. K., in preparation, Automatic generation of ground-water flow nets using numerical models: The University of Texas at Austin, Bureau of Economic Geology.

Freeze, R. A., and Cherry, J. A., 1979, Ground water: Englewood Cliffs, N. J., Prentice Hall, 604 p.

- Gustavson, T. C., Presley, M. W., Handford, C. R., Finley, R. J., Dutton, S. P., Baumgardner, R. W., Jr., McGillis, K. A., and Simpkins, W. W., 1980c, Geology and geohydrology of the Palo Duro Basin, Texas Panhandle--A report on the progress of nuclear waste isolation feasibility studies (1979): The University of Texas at Austin, Bureau of Economic Geology Geological Circular 80-7, 99 p.
- Handford, C. R., 1980, Lower Permian facies of the Palo Duro Basin, Texas: depositional systems, shelf-margin evolution, paleogeography, and petroleum potential: The University of Texas at Austin, Bureau of Economic Geology Report of Investigations No. 102, 31 p.
- Handford, C. R., and Dutton, S. P., 1980, Pennsylvanian-Lower Permian depositional systems and shelf-margin evolution, Palo Duro Basin, Texas: American Association of Petroleum Geologists Bulletin, v. 64, no. 1, p. 88-106.
- Handford, C. R., Dutton, S. P., and Fredericks, P. E., 1981, Regional cross sections of the Texas Panhandle: Precambrian to Mid-Permian: The University of Texas at Austin, Bureau of Economic Geology.
- INTERA, 1983, First status report on regional ground-water flow modeling for the Palo Duro Basin, Texas: ONWI/E512-02900/TR-13.
- Knowles, T., Nordstrom, P., and Klemm, W. B., 1982, Evaluating ground water resources of the High Plains of Texas, Final Report: Texas Department of Water Resources, LP-173.

Kreitler, C. W., and Bassett, R. L., 1983, Chemical and isotopic composition of saline ground water and saline springs in the Rolling Plains east of the Ogallala Escarpment, in Gustavson, T. C., and others, Geology and geohydrology of the Palo Duro Basin, Texas Panhandle, a report on the progress of nuclear waste isolation feasibility studies: The University of Texas at Austin, Bureau of Economic Geology Geological Circular 83-4.

McGowen, J. H., 1981, Depositional sequences and associated sedimentary diagenetic facies: an ongoing investigation of salt-bearing core, Swisher County, Texas, in Gustavson, T. C., and others, Geology and geohydrology of the Palo Duro Basin, Texas Panhandle, a report on the progress of nuclear waste isolation feasibility studies (1980): The University of Texas at Austin, Bureau of Economic Geology Geological Circular 81-3, p. 90-92.

McGowen, J. H., Granata, G. E., and Seni, S. J., 1979, Depositional framework of the lower Dockum Group (Triassic), Texas Panhandle: The University of Texas at Austin, Bureau of Economic Geology Report of Investigations No. 97, 60 p.

Mower, R. W., Hood, J. W., and Cushman, R. L., 1964, An appraisal of potential ground water salvage along the Pecos River between dome and artesia: U. S. Geological Survey Water Supply Paper 1659.

Myers, B. N., 1969, Compilation of results of aquifer tests in Texas: Texas Water Development Board Report No. 98, 532 p.

Neuman, S. P., 1976, User's Guide for FREESURF: Department of Hydrology and Water Resources, University of Arizona, Tucson, Arizona.



- Neuman, S. P., and Witherspoon, P. A., 1970, Finite element method of analyzing steady seepage with a free surface: *Water Resources Research*, v. 6, no. 3, p. 889-897.
- Orr, E. D., 1984, Investigation of underpressuring in the Deep-Basin Brine Aquifer, Palo Duro Basin: The University of Texas at Austin, Bureau of Economic Geology Open-File Report OF-WTWI-1984-6, 20 p.
- Richter, B. C., 1983, Geochemical and hydrogeological characteristics of salt springs and shallow subsurface brines in the Rolling Plains of Texas and southwest Oklahoma: The University of Texas at Austin, Master's thesis, 147 p.
- Senger, R. K., and Fogg, G. E., 1983, Regional modeling of ground water flow in the Palo Duro Basin, Texas Panhandle, in Gustavson, T. C., and others, *Geology and geohydrology of the Palo Duro Basin, Texas Panhandle--A report on the progress of nuclear waste isolation feasibility studies*: The University of Texas at Austin, Bureau of Economic Geology Geological Circular 83-4.
- Senger, R. K., Richter, B. C., and Kreitler, C. W., in preparation, Isotopic composition of shallow ground waters in eastern New Mexico and Texas Panhandle, in Gustavson, T. C., and others, *Geology and geohydrology of the Palo Duro Basin, Texas Panhandle--A report on the progress of nuclear waste isolation feasibility studies (1983)*: The University of Texas at Austin, Bureau of Economic Geology Geological Circular.
- Seni, S. J., 1977, Hydrochemical facies of the Texas Panhandle: unpublished manuscript, 52 p.

\_\_\_\_\_, 1980, Sand-body geometry and depositional systems, Ogallala Formation, Texas: The University of Texas at Austin, Bureau of Economic Geology Report of Investigations No. 105, 36 p.

Smith, D. A., 1983, Permeability of the Deep-Basin Brine Aquifer System, Palo Duro Basin, in Gustavson, T. C., and others, Geology and geohydrology of the Palo Duro Basin, Texas Panhandle--a report on the progress of nuclear waste isolation feasibility studies: The University of Texas at Austin, Bureau of Economic Geology Geological Circular 83-4.

Smith, D. A., in preparation, Potentiometric surface of the Upper Pennsylvanian Aquifer, in Gustavson, T. C., and others, Geology and Geohydrology of the Palo Duro Basin, Texas Panhandle--A report on the progress of nuclear waste isolation feasibility studies: The University of Texas at Austin, Bureau of Economic Geology.

Stone and Webster Engineering Corporation, 1983, Hydrogeologic investigations based on drill-stem test data, Palo Duro Basin area, Texas and New Mexico: Topical Report.

Summers, W. K., 1981, Ground-water head distribution in the third dimension of the Pecos River Basin, New Mexico: New Mexico Geology.

Wirojanagud, P., Kreitler, C. W., and Smith, D. A., 1984, Numerical modeling of regional ground-water flow in the Deep-Brine Aquifers of the Palo Duro Basin, Texas Panhandle: The University of Texas at Austin, Bureau of Economic Geology Open-File Report: OF-WTWI-1984-8.

## FIGURE CAPTIONS

Figure 1. Structural features of Texas Panhandle and adjacent areas (modified from Handford, 1980).

Figure 2. Regional east-west cross section illustrating spatial relationships of the major depositional systems in the Palo Duro Basin (after Bassett and others, 1981).

Figure 3. Potentiometric head map of the unconfined aquifers that overlie the evaporite sequences (after Bassett and others, 1981).

Figure 4. Potentiometric head map of the whole Deep-Basin Brine Aquifer constructed from kriged estimates of heads (after Wirojauagud and others, in preparation).

Figure 5. Difference in hydraulic heads between unconfined aquifer and Deep-Basin Brine Aquifer (after Wirojanagud and others, in preparation).

Figure 6. Finite Element Mesh representing the major hydrologic units. Each element is assigned a hydraulic conductivity value according to the different simulations. Numbered labels on the elements correspond to geologic facies listed in table 4. The upper surface of the mesh is represented with prescribed head boundary conditions and prescribed flux boundary conditions (High Plains surface) and reflect the water table conditions. Heads are assumed to be uniform with depth along the eastern boundary. The lower surface of the mesh is a no-flow boundary which corresponds to the contact between the Deep-Basin Brine Aquifer and basement rock.

Figure 7. Pressure-depth data from the Deep-Basin Brine Aquifer, Jackson County, Oklahoma, which is located approximately at the eastern edge of the cross section. The pressure-depth regression line has a slope equivalent to brine hydrostatic.

Figure 8. Simulation A-1 of computed hydraulic head distribution with hydraulic conductivities from table 4. Hydraulic heads beneath the Evaporite Aquitard are lower by up to 300 m (1000 ft) than unconfined heads. East of the Caprock Escarpment, however, hydraulic heads in the Deep-Basin Brine Aquifer are unrealistically high.

Figure 9. Simulation A-2 of computed hydraulic head distribution with increased permeability of proximal granite wash. It shows that subhydrostatic conditions prevail in the Deep-Basin Brine Aquifer east of the escarpment.

Figure 10. Isolith map of Pennsylvanian and Wolfcampian granite wash in the Texas Panhandle (after Dutton and others, 1982).

Figure 11. Streamline distribution according to Simulation A-2. Ground-water flow is concentrated in the shallow aquifer system. Only a small fraction of flow is passing through the Deep-Basin Brine Aquifer.

Figure 12. Simulation A-3 of computed hydraulic head distribution with increased hydraulic conductivities for granite wash compared to Simulation A-2. It shows increased depressuring towards the western part of the Deep-Basin Brine Aquifer.

Figure 13. Streamline distribution according to Simulation A-3. Ground-water flow pattern within the Deep-Basin Brine Aquifer is governed primarily by the spatial distribution of relatively permeable granite-wash deposits.

Figure 14. Simulation B-1 of computed hydraulic head distribution with increased vertical permeability of the Evaporite Aquitard. It shows a drastic head increase in the deep section.

Figure 15. Simulation B-2 of computed hydraulic head distribution with decreased vertical permeability of the Evaporite Aquitard. It shows a general decrease of heads in the Deep-Basin Brine Aquifer by up to 50 m (164 ft) in the central part of the cross section.

Figure 16. Simulation C of computed hydraulic head distribution with modified finite element mesh. It shows increased heads in the western part of the cross section. In the eastern part, however, extensive subhydrostatic conditions are maintained.

Figure 17. Streamline distribution according to Simulation C. Ground-water flow into the Deep-Basin Brine Aquifer increased from 0.0034 (Simulation A-2) to 0.047 m<sup>3</sup>/day.

Figure 18. Simulation D of computed hydraulic head distribution considering vertical head differential within the shallow aquifer system. Hydraulic heads in the deep section are not significantly changed compared to heads in Simulation A-2.

Figure 19. Streamline distribution according to Simulation D. The general ground-water flow pattern appears not to be affected by the vertical head differential in the

Dockum. Vertical leakage through the Evaporite Aquitard, however, is reduced by about 19 percent compared to Simulation A-2.

#### APPENDIX FIGURES

Figure A1. Simplified model to test the effect of node spacing differences in horizontal and vertical direction.

Figure A2. Diagram showing the differences in computed hydraulic heads at the corresponding node locations with respect to the 4-element case.



## TABLE CAPTIONS

Table 1. Generalized stratigraphic column of the Palo Duro Basin (modified from Bassett and Bentley, 1983).

Table 2. Permeability of individual hydrogeologic units of Palo Duro Basin (after Wirojanagud, in preparation).

Table 3. Summary of numerical simulations of the cross-sectional ground-water flow model.

Table 4. Assigned hydraulic conductivity values for the major hydrologic systems.

## APPENDIX TABLE

Table A1. Performance of the simplified model at different conductance ratios.

## Appendix A

### Effect of Node Spacing Differences in Horizontal and Vertical Direction on the Hydraulic Head Solution

Anisotropic node spacing in numerical models can cause significant numerical errors in the solution of hydraulic head. Typical horizontal and vertical node spacings in the present model are 12,300 m (40,350 ft) and 250 m (820 ft), respectively. To test the effects of anisotropic node spacing on hydraulic heads computed by the program "FREESURF," several numerical experiments were run.

Finite element grids were set up with 4, 50, 100, and 200 elements with each mesh having the same total size. Each finite element mesh consists of three columns of nodes and each is subdivided horizontally to obtain 4, 5, 100, or 200 elements in successive simulations (fig. A1).

The boundary conditions of the model are such that the upper left node #3 has a prescribed head of 100 m (330 ft), and the lower right node #7 has a prescribed head of 0 m (0 ft). Boundary conditions on all other nodes are no-flow (prescribed flux equal to zero). The finite difference grid has a total size of 5,000 m (16,400 ft) in horizontal direction and 2,500 m (8,200 ft) in vertical direction. The size for each individual element for the various cases ranges from 2,500 m (8,200 ft) x 1,250 m (4,100 ft) (4-element case), 2,500 m (8,200 ft) x 100 m (330 ft) (50-element case), 2,500 m (8,200 ft) x 50 m (165 ft) (100-element case) to 2,500 m (8,200 ft) x 25 m (82 ft) (200-element case).

The hydraulic head distribution was simulated under two different hydrologic conditions:

1. isotropic, homogeneous conditions with  $K_x = K_y = 30$  m/day
2. anisotropic, homogeneous conditions with  $K_x = 30$  m/day and  $K_y = 3,000$  m/day

The difference in horizontal and vertical node affects the conductance term (C), which represents the rate of fluid transfer due to a unit difference in hydraulic head between two nodes:

$$C = K \times A/dl$$

where: K is the hydraulic conductivity  
A is the cross-sectional area  
dl is the distance between two nodes

For the mesh with 200 elements the ratio between the C value in y-direction and x-direction becomes  $10^4$  for the isotropic, homogeneous condition ( $C_x = 0.3$ ,  $C_y = 3,000$ ) and increases to  $10^6$  for the anisotropic, homogeneous condition ( $C_x = 0.3$ ,  $C_y = 300,000$ ). In comparison, the conductance rate for an average element of the cross sectional model (fig. 6) is  $C_y/C_x = 2,420$  for isotropic conditions, and  $C_y/C_x = 242,000$  for anisotropic conditions with  $K_y/K_x = 100$ .

The computed hydraulic heads at the corresponding node locations for the different simulations were compared and the differences in head, respectively, to the 4-element case are shown in figure A2. Additionally, the overall performance of the different simulations is listed in table A1. The 4-element case can be considered the true solution. The errors in computed hydraulic head are small and can be considered negligible for most practical purposes. Hence, the anisotropic node spacing in the present model does not cause significant numerical errors.

Table 1. Generalized stratigraphic column of the Palo Duro Basin  
(modified from Bassett and Bentley, 1983).

System	Series	Group	General lithology and depositional setting	Hydrogeologic element	Hydrogeologic unit
Quaternary			Fluvial and lacustrine clastics		
Tertiary				Ogallala aquifer	Shallow aquifer
Cretaceous			Nearshore marine clastics		
Triassic		Dockum	Fluvial deltaic and lacustrine clastics and limestones	Dockum aquifer	
Permian	Ochoa	Artesia	Salt, anhydrite, red beds and peritidal dolomite	Evaporite Aquitard	Evaporite Aquitard
	Guadalupe	Pease River			
	Leonard	Clear Fork			
		Wichita			
Pennsylvanian	Wolfcamp		Shelf and platform carbonates, basin shale and deltaic sandstones	Wolfcamp carbonate aquifer	Wolfcamp carbonate
				Pennsylvanian carbonate aquifer	Deep-Basin Brine Aquifer
				Upper Paleozoic granite wash aquifer	Wolfcamp granite wash
			Basin shale		Basin shale
Mississippian			Shelf limestone and chert		Pennsylvanian carbonate
				Lower Paleozoic carbonate aquifer	Pennsylvanian granite wash
Ordovician		Ellenburger	Shelf dolomite		
Cambrian			Shallow marine (?) sandstone	Lower Paleozoic sandstone aquifer	
	Precambrian		Igneous and metamorphic	Basement aquiclude	Pre-Pennsylvanian-age rock
					Basement aquiclude

Table 2. Permeability of individual hydrogeologic units of Permian and Pennsylvanian of the Palo Duro Basin (after Wirojanagud and others, 1984).

Hydrogeologic unit	$y = \ln(k)$		Geometric mean of $k$ (eY), md	Number and source of data	Typical value md
	Average value, $y$	Variance, $s^2$			
Evaporite strata	---	---	---	---	.00028++ (vertical permeability)
Deep brine aquifer	Wolfcampian carbonate	2.19	5.08	8.90	25 - DST data 70 - Core Lab Inc. (1972) 6 - Sawyer #1 pumping test data
	Pennsylvanian carbonate	2.88	5.61	17.90	25 - DST data 118 - Core Lab Inc. (1972)
	shale	---	---	---	.0001 + .00001------.08*
	granite wash	2.15 (1.27 with Mobeetie data)	7.13	8.60 (3.55 with Mobeetie data)	10 - DST data 10 - Sawyer #1 pumping test 415 - Mobeetie field core data 11 - Core Lab Inc. (1972)
Pre-Pennsylvanian rock	1.56	5.70	4.76	11 - DST data 14 - Sawyer #1 pumping test data	.01-----380* ---

\* range of permeability, from Davis and DeWiest (1966), Davis (1980), Freeze and Cherry (1979)  
+ average permeability, assigned to basinal system (fig. 2)

++ derived from the harmonic means of permeabilities using typical or measured values of permeability for each substrata



Table 3. Summary of numerical simulations of the cross-sectional ground-water flow model.

Conditions	A1	A2	A3	B1	B2	C	D
1. Granite Wash (GW) Permeability:							
uniform GW: $k = 8.6$ md	X						
distal GW: $k = 8.6$ md							
proximal GW: $k = 100$ md (east of escarpment)		X		X	X	X	X
distal GW: $k = 100$ md (extended into NM)							
proximal GW: $k = 250$ md (east of escarpment)			X				
2. Role of Evaporite Aquitard							
$k = 2.8 \times 10^{-3}$ md				X			
$k = 2.8 \times 10^{-4}$ md	X	X	X			X	X
$k = 2.8 \times 10^{-9}$ md					X		
3. Hydraulic Interconnection of Ogallala and Dockum							
Ogallala/Dockum aquifer: $K_X/K_Z = 10$	X	X	X	X	X	X	
Ogallala aquifer: $K_X/K_Z = 100$							X
Dockum aquifer: $K_X/K_Z = 10,000$							X
4. Effect of Pecos River						X	

Table 4. Assigned hydraulic conductivity values for the major hydrologic systems.

Hydrologic Unit	Hydraulic Conductivity (m/day)	
	horizontal ( $K_x$ )	vertical ( $K_z$ )
1. Ogallala fluvial system <sup>1</sup>	$8.0 \times 10^0$	$8.0 \times 10^{-1}$
2. Triassic fluvial/lacustrine system <sup>1</sup>	$8.0 \times 10^{-1}$	$8.0 \times 10^{-2}$
3. Permian (salt dissolution zone) <sup>3</sup>	$8.2 \times 10^{-2}$	$8.2 \times 10^{-4}$
4. Permian sabkha system <sup>4</sup>	$3.2 \times 10^{-7}$	$3.2 \times 10^{-7}$
5. Permian mudflat system <sup>2</sup>	$8.2 \times 10^{-5}$	$8.2 \times 10^{-5}$
6. Permian/Pennsylvanian shelf carbonates <sup>4</sup>	$1.3 \times 10^{-2}$	$1.3 \times 10^{-4}$
7. Permian/Pennsylvanian basinal systems <sup>4</sup>	$1.1 \times 10^{-7}$	$1.0 \times 10^{-7}$
8. Permian/Pennsylvanian mudflat and alluvial/fan delta system <sup>2</sup>	$8.2 \times 10^{-2}$	$8.2 \times 10^{-4}$
9. Permian/Pennsylvanian fan delta system (granite wash) <sup>4</sup>	$1.0 \times 10^{-2}$	$1.0 \times 10^{-4}$

Sources of data:

1.  $K_x$  from Myers (1969); assumed  $K_x/K_z = 10$
2. typical value of geologic material (Freeze and Cherry, 1979)
3.  $K_x$  from U.S. Geological Survey open-file data; assumed  $K_x/K_z = 100$
4. after Table 2

Table A1. Performance of the model at different conductance ratios.

1. isotropic system:  $K_x = K_y = 30$  m/day

	Total discharge (#7)	Mass Balance (%)*	Conductance Ratio $C_y/C_x$
4 elements	887.8049	$-.123 \times 10^{-11}$	4
50 elements	844.4009	$-.162 \times 10^{-9}$	625
100 elements	844.1807	$+.149 \times 10^{-7}$	2,500
200 elements	844.1807	$-.149 \times 10^{-7}$	10,000

2. anisotropic:  $K_x = 30$  m/day  $K_y = 3,000$  m/day

	Total discharge (#7)	Mass Balance (%)*	Conductance Ratio $C_y/C_x$
4 elements	1486.432	$-.266 \times 10^{-9}$	400
50 elements	1485.612	$-.241 \times 10^{-6}$	62,500
100 elements	1485.609	$.160 \times 10^{-6}$	250,000
200 elements	1485.607	$-.357 \times 10^{-5}$	1,000,000

\*Mass balance =  $\frac{(\text{inflow} - \text{outflow})}{\text{inflow}} \times 100$

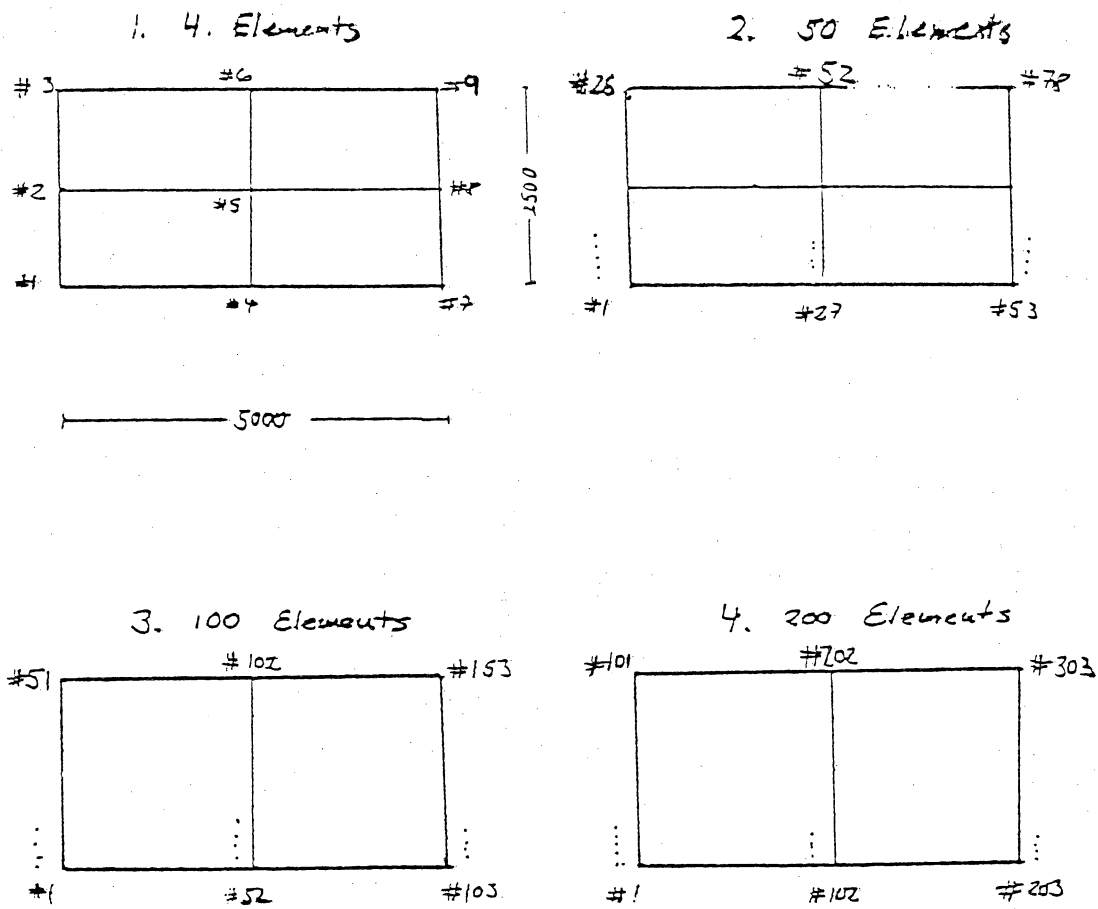
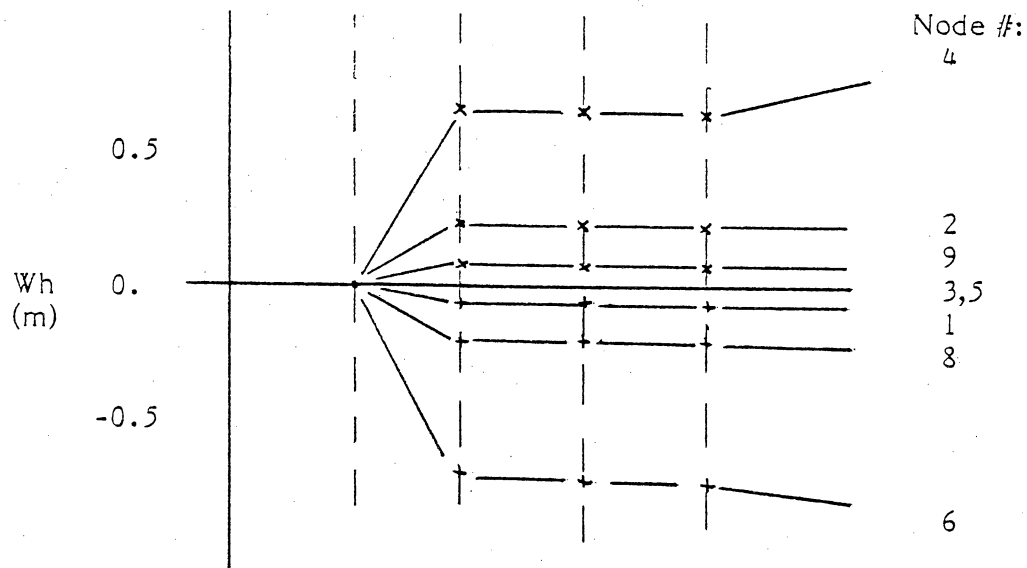


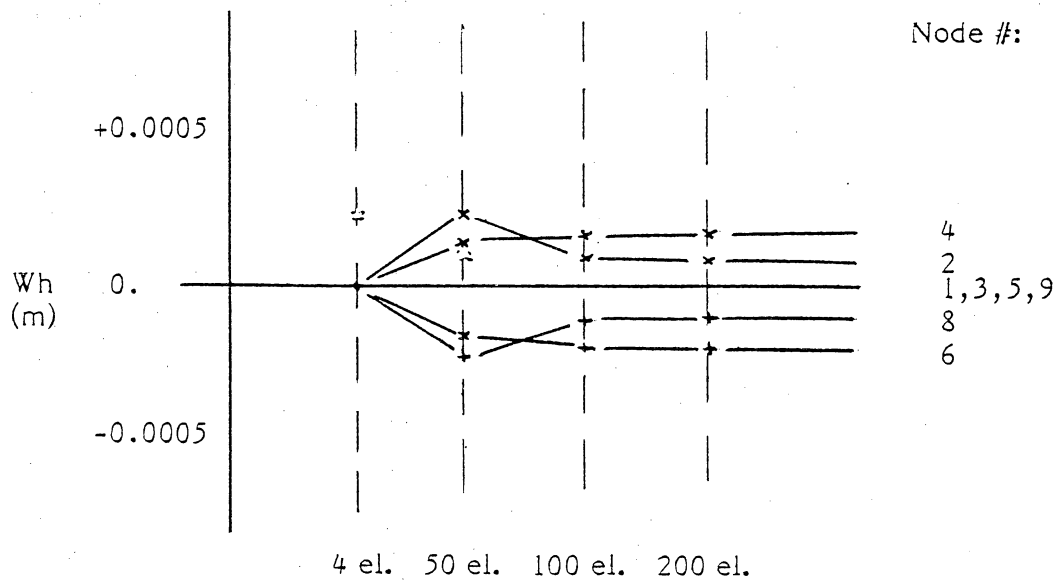
Figure A1. Simplified model to test the effect of node spacing differences in horizontal and vertical direction.

Figure A2. Diagram showing the differences in computed hydraulic heads at the corresponding node locations with respect to the 4-element case.

a. isotropic homogeneous conditions



b. anisotropic homogeneous conditions





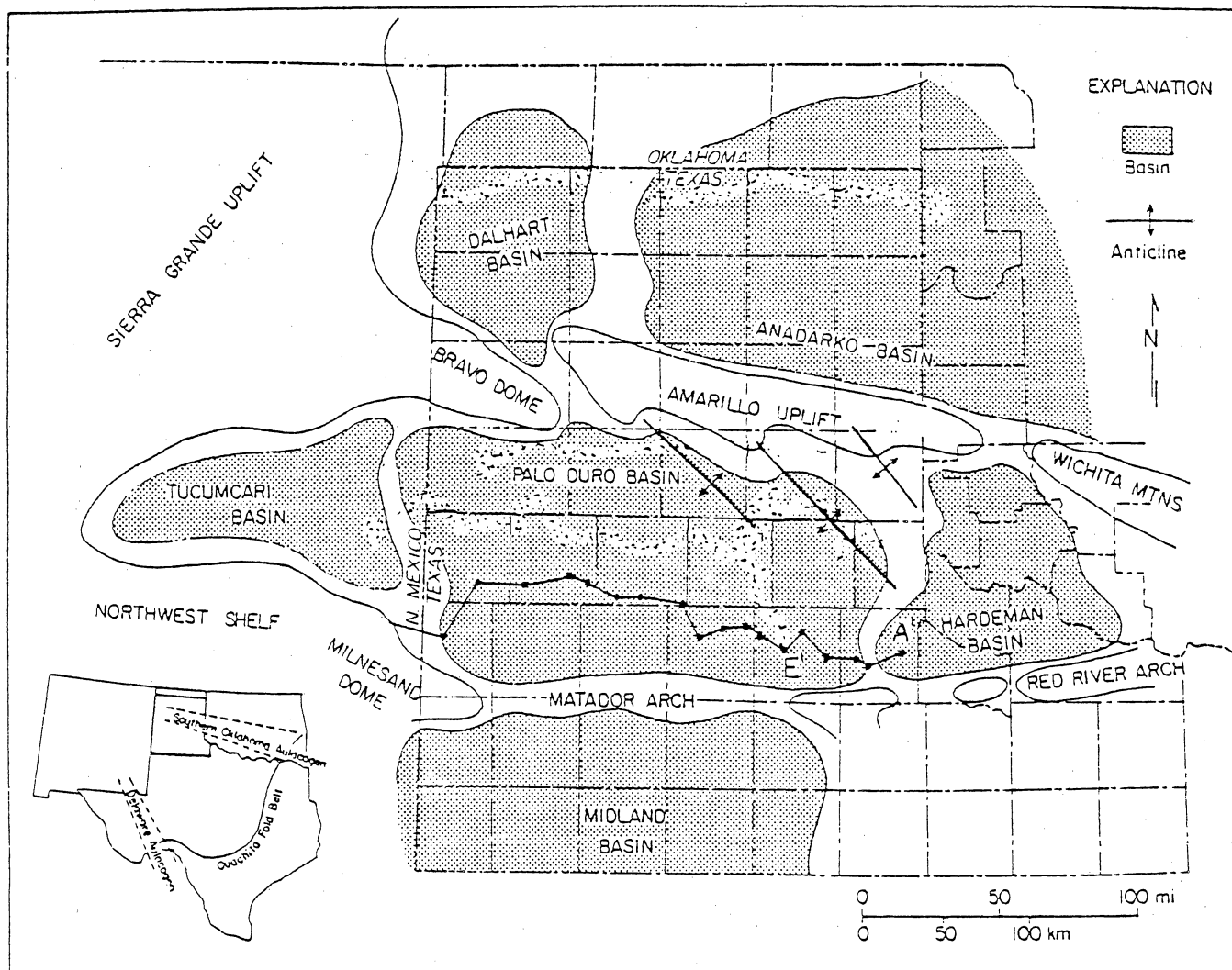


Figure 1. Structural features of Texas Panhandle and adjacent areas (modified from Handford, 1980).

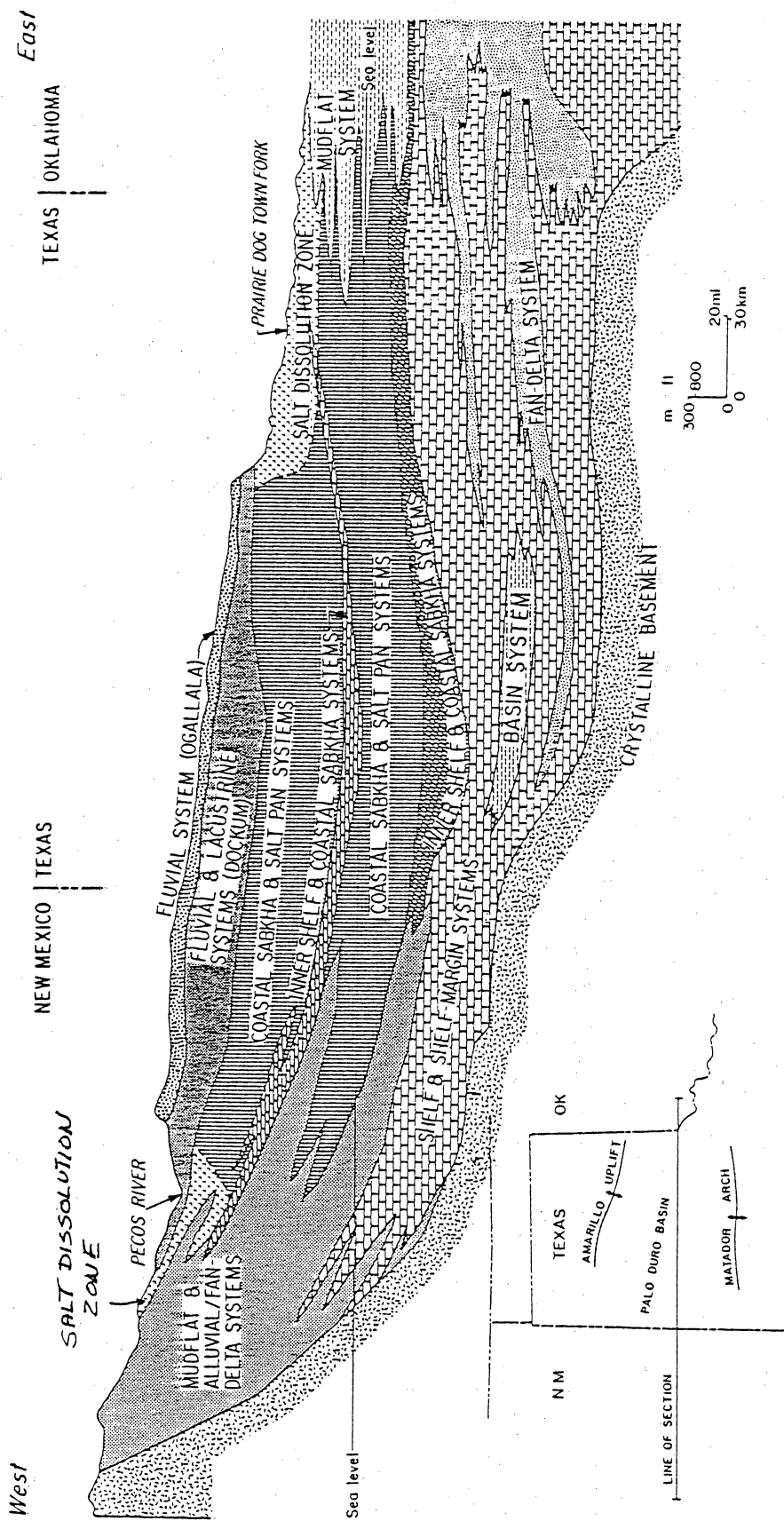


Figure 2. Regional east-west cross section illustrating spatial relationships of the major depositional systems in the Palo Duro Basin (after Bassett and others, 1981).

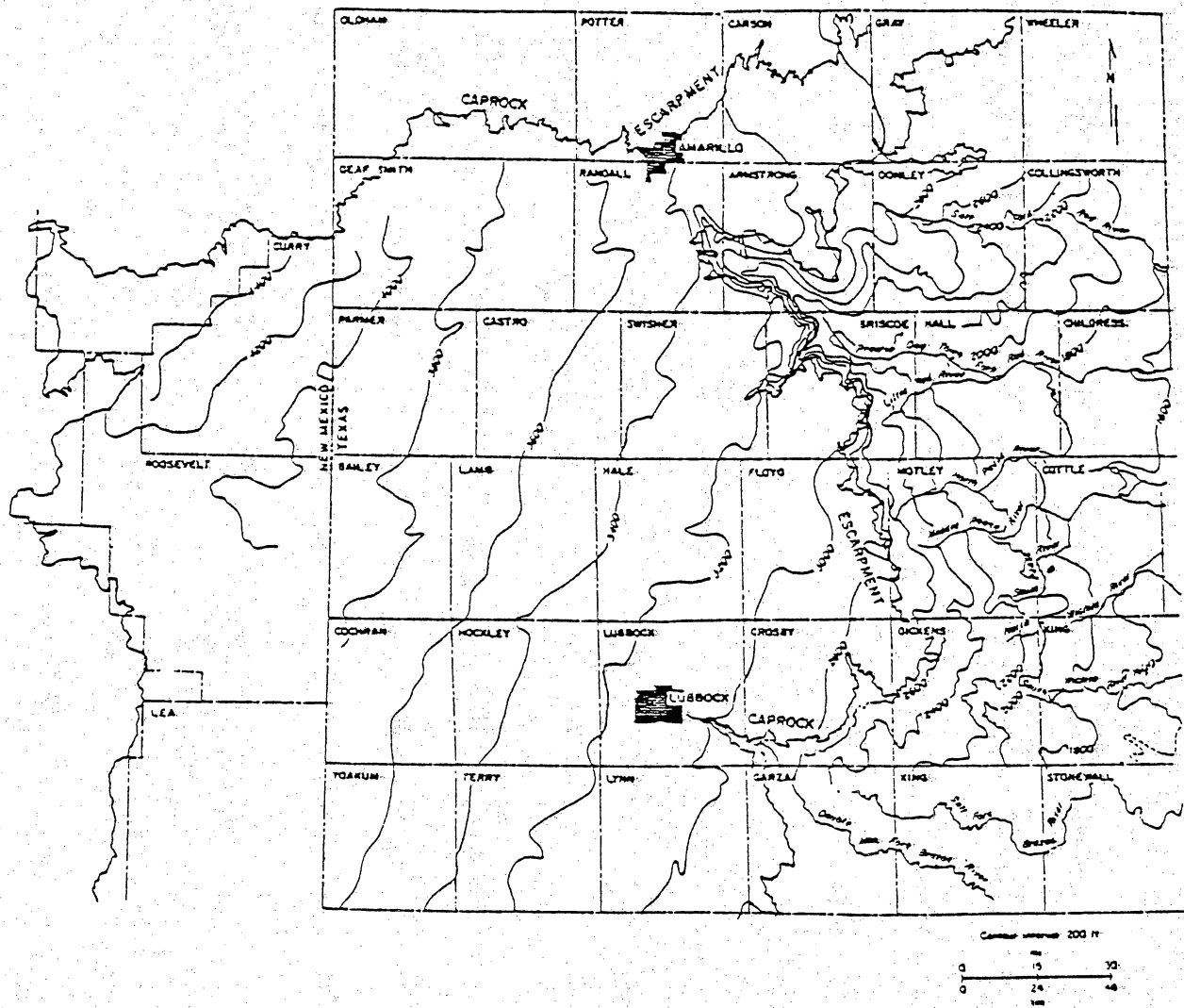
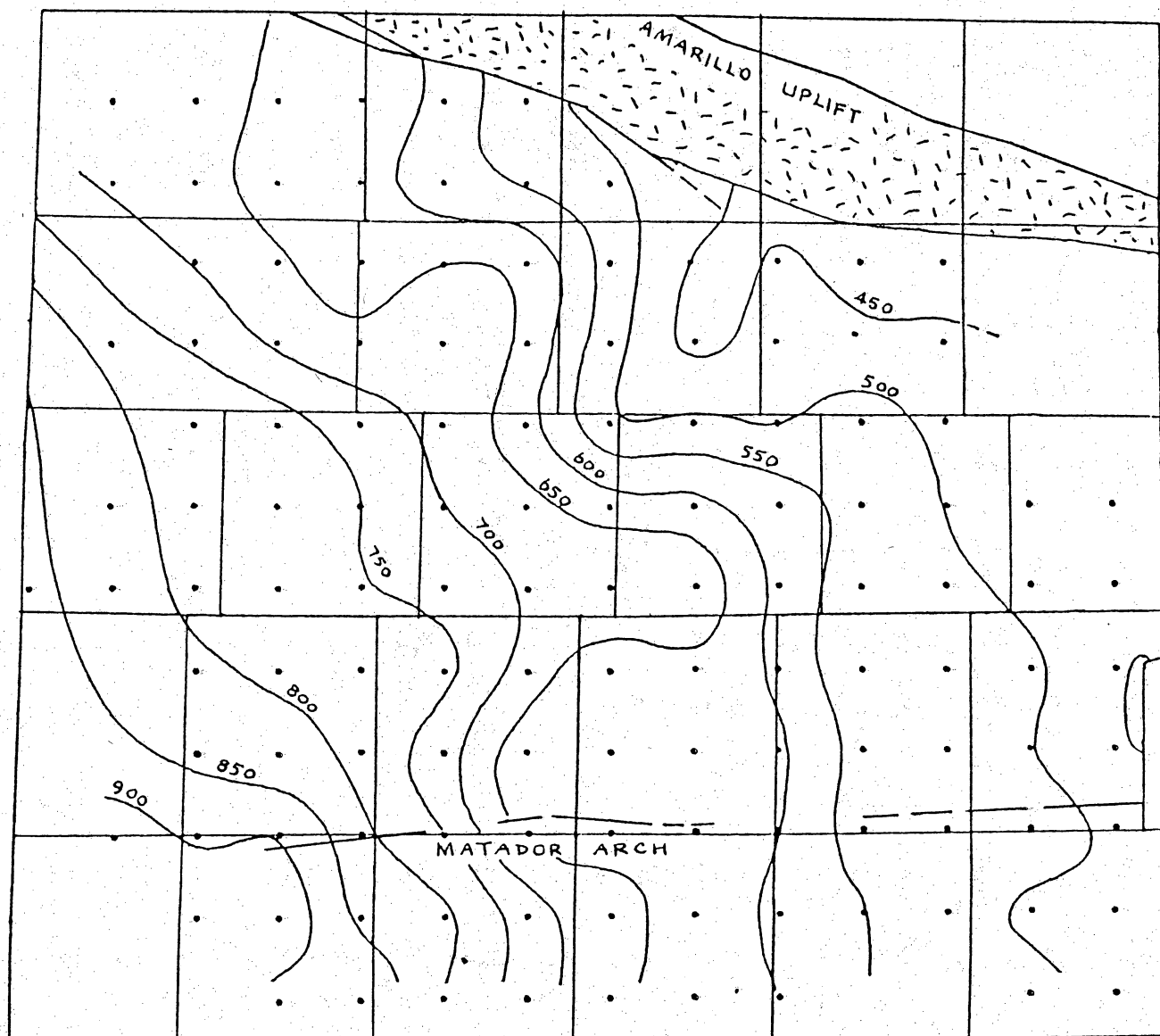


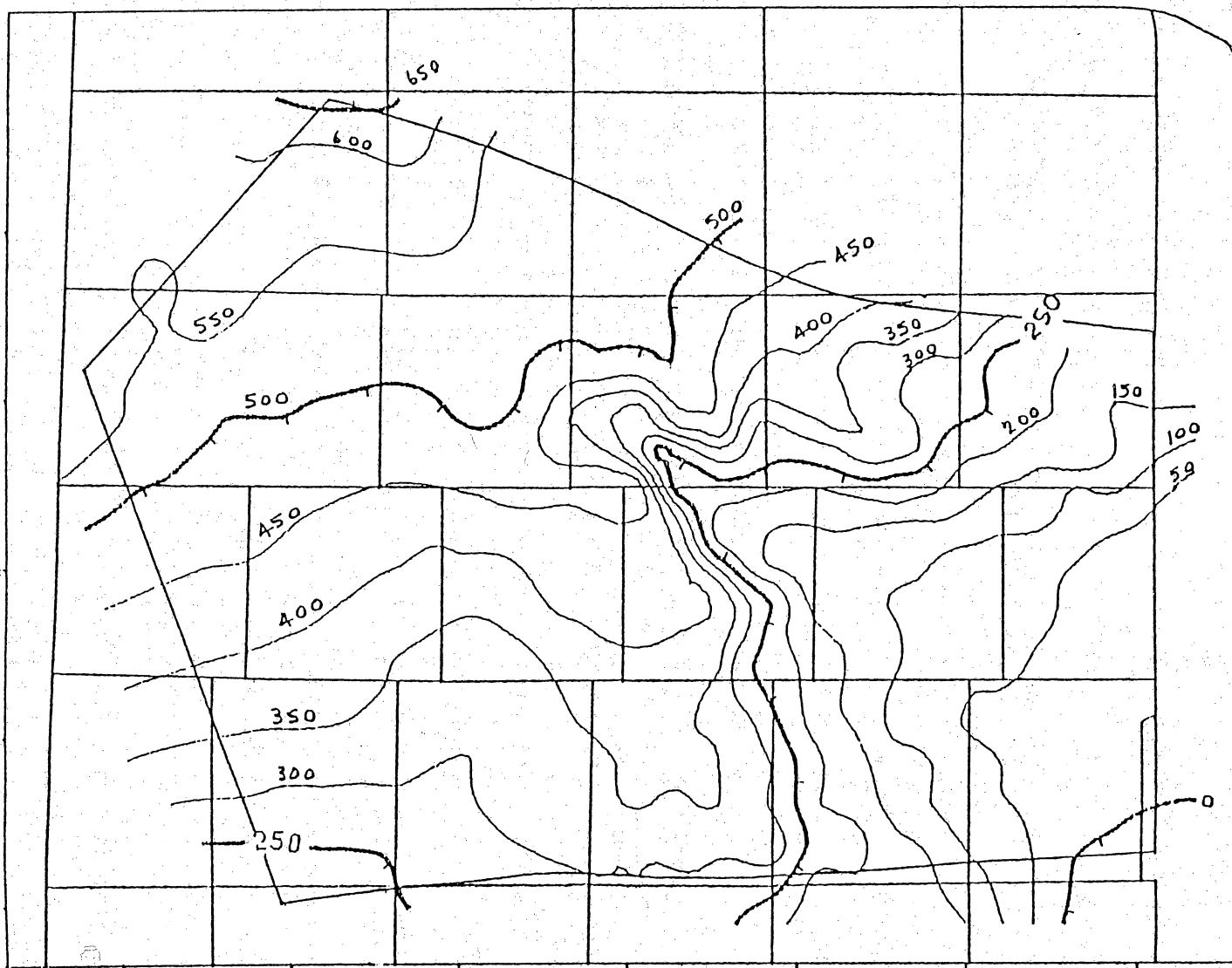
Figure 3. Potentiometric head map of the unconfined aquifers that overlie the evaporite sequences (after Bassett and others, 1981).



Contour Interval = 50m

● Kriged Point

Figure 4. Potentiometric head map of the whole Deep-Basin Brine Aquifer constructed from kriged estimates of heads (after Wirojanagud and others, in preparation).



Contour Interval = 50m

Figure 5. Difference in hydraulic heads between unconfined aquifer and Deep-Basin Brine Aquifer (after Wirojanagud and others, in preparation).

(Labels correspond to geologic facies in Table 4).

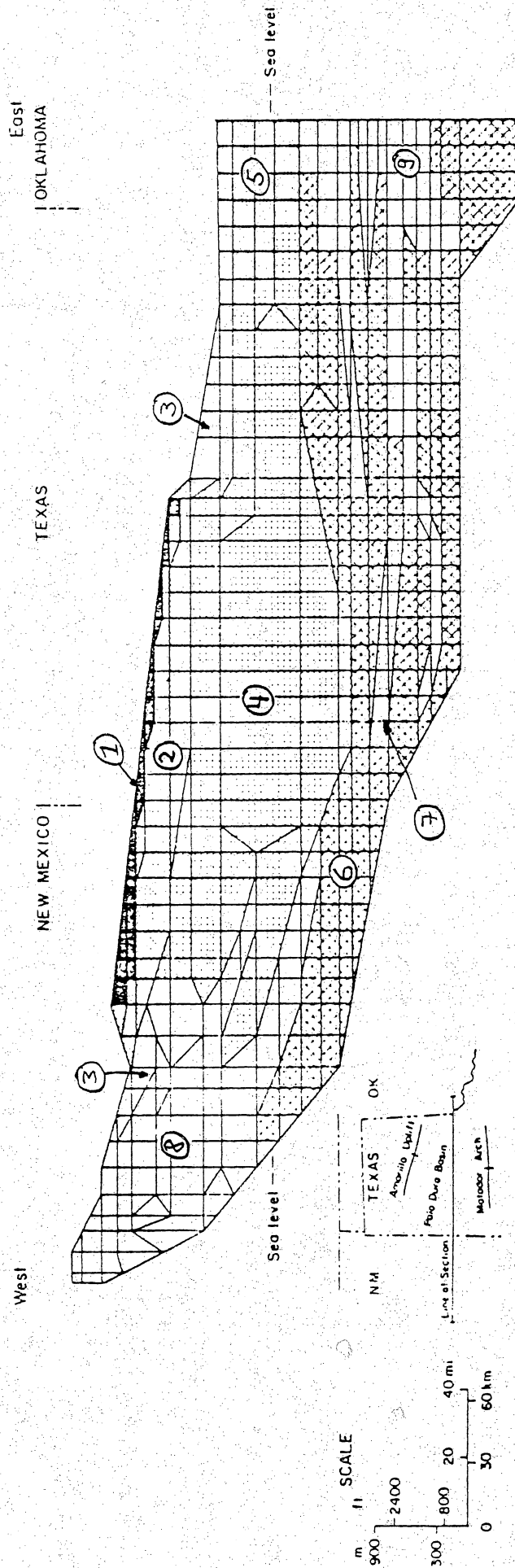


Figure 6. Finite Element Mesh representing the major hydrologic units. Each element is assigned a hydraulic conductivity value according to the different simulations. Numbered labels on the elements correspond to geologic facies listed in Table 4. The upper surface of the mesh is represented with prescribed head boundary conditions and prescribed flux boundary conditions (High Plains surface) and reflect the water table conditions. Heads are assumed to be uniform with depth along the eastern boundary. The lower surface of the mesh is a no-flow boundary which corresponds to the contact between the Deep-Basin Brine Aquifer and basement rock.



## JACKSON COUNTY

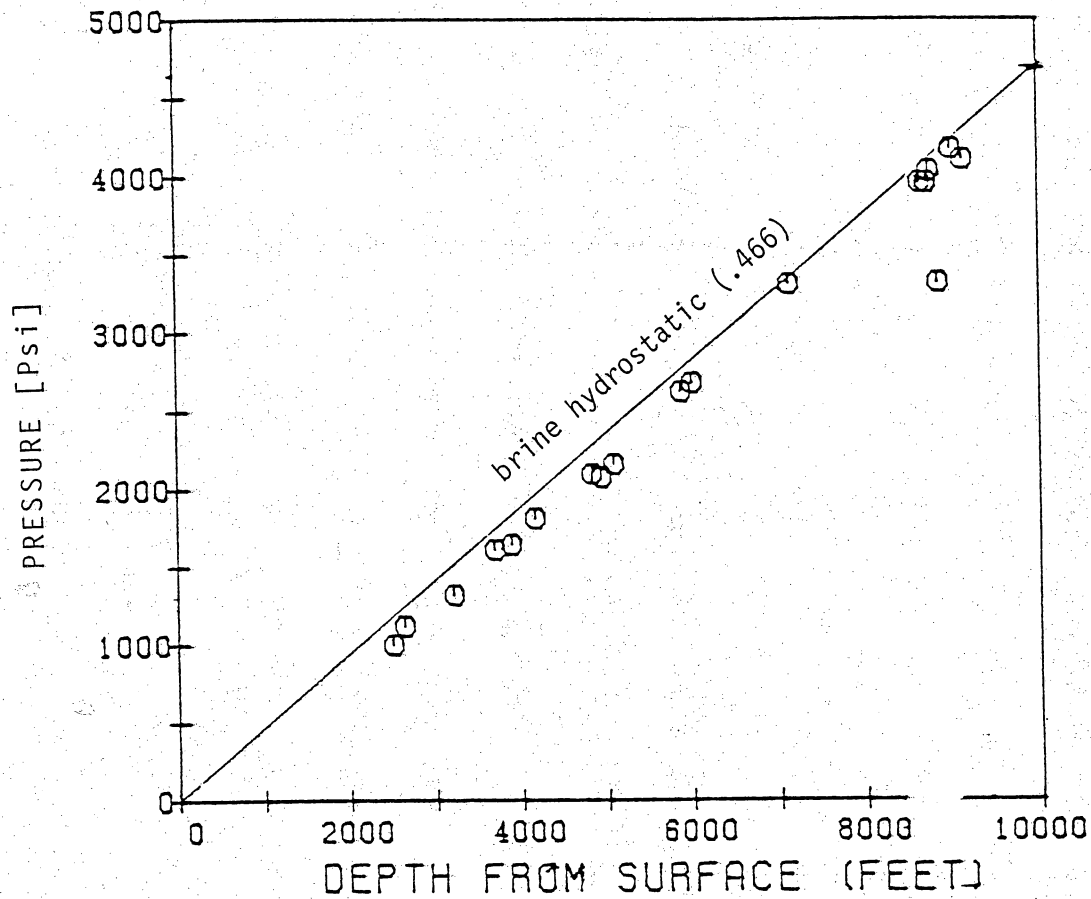
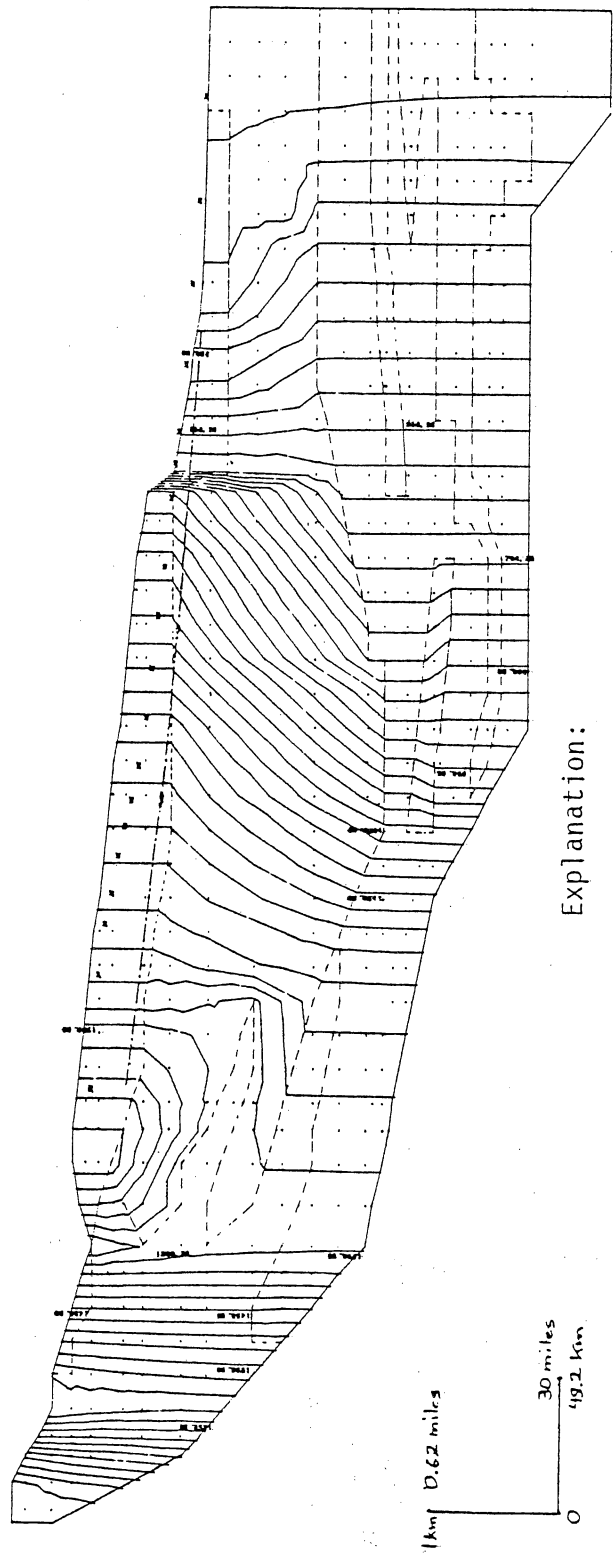


Figure 7. Pressure-depth data from the Deep-Basin Brine Aquifer, Jackson County, Oklahoma, which is located approximately at the eastern edge of the cross section. The pressure-depth regression line has a slope equivalent to brine hydrostatic.

West N.Hx. | Tx Tx | Okla. East



Explanation:

- Interval of head contour: 25m
- - - - - Approximated heads based on kriged head map (fig. 4)
- x x x Computed potentiometric surface of Deep-Basin Brine Aquifer
- - - - - Distribution of different geologic facies

Figure 8. Simulation A-1 of computed hydraulic head distribution with hydraulic conductivities from Table 4. Hydraulic heads beneath the Evaporite Aquitard are lower by up to 300m (1000ft) than unconfined heads. East of the Caprock Escarpment, however, hydraulic heads in the Deep-Basin Brine Aquifer are unrealistically high.

West  $N.H_{xc}$   $T_x$   $T_x$   $Okla.$  East

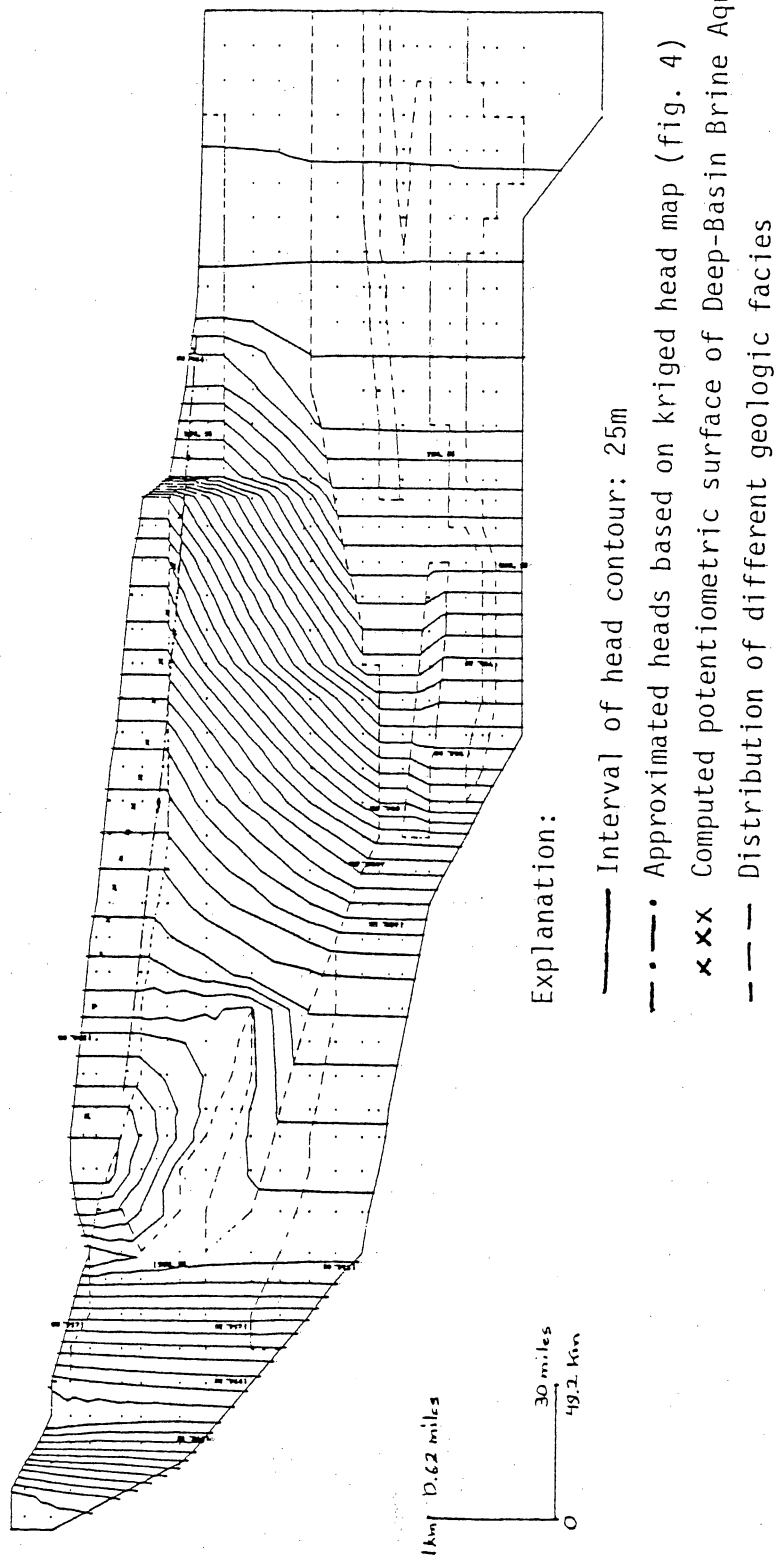


Figure 9. Simulation A-2 of computed hydraulic head distribution with increased permeability of proximal granite wash. It shows that subhydrostatic conditions prevail in the Deep-Basin Brine Aquifer east of the escarpment.

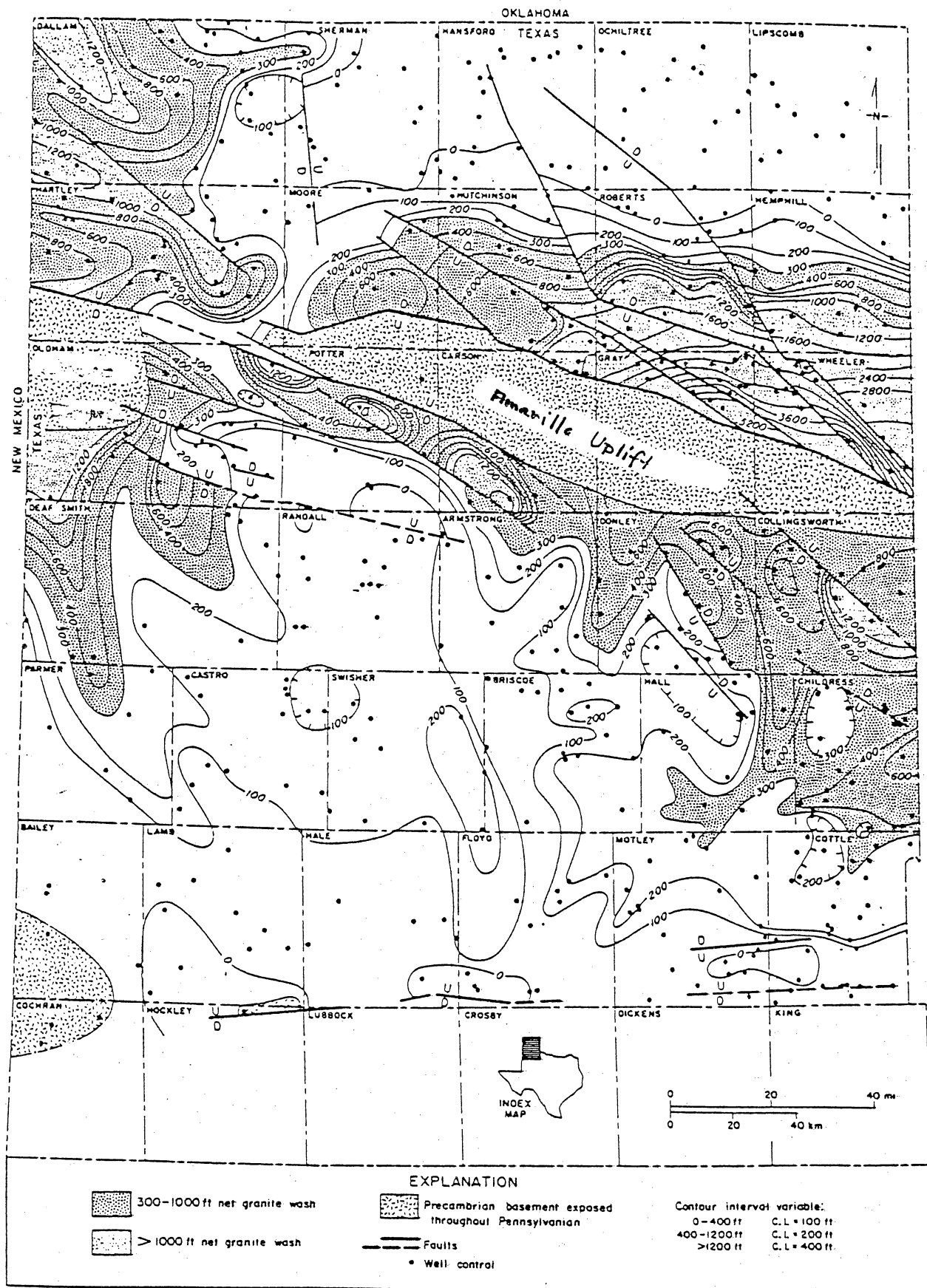
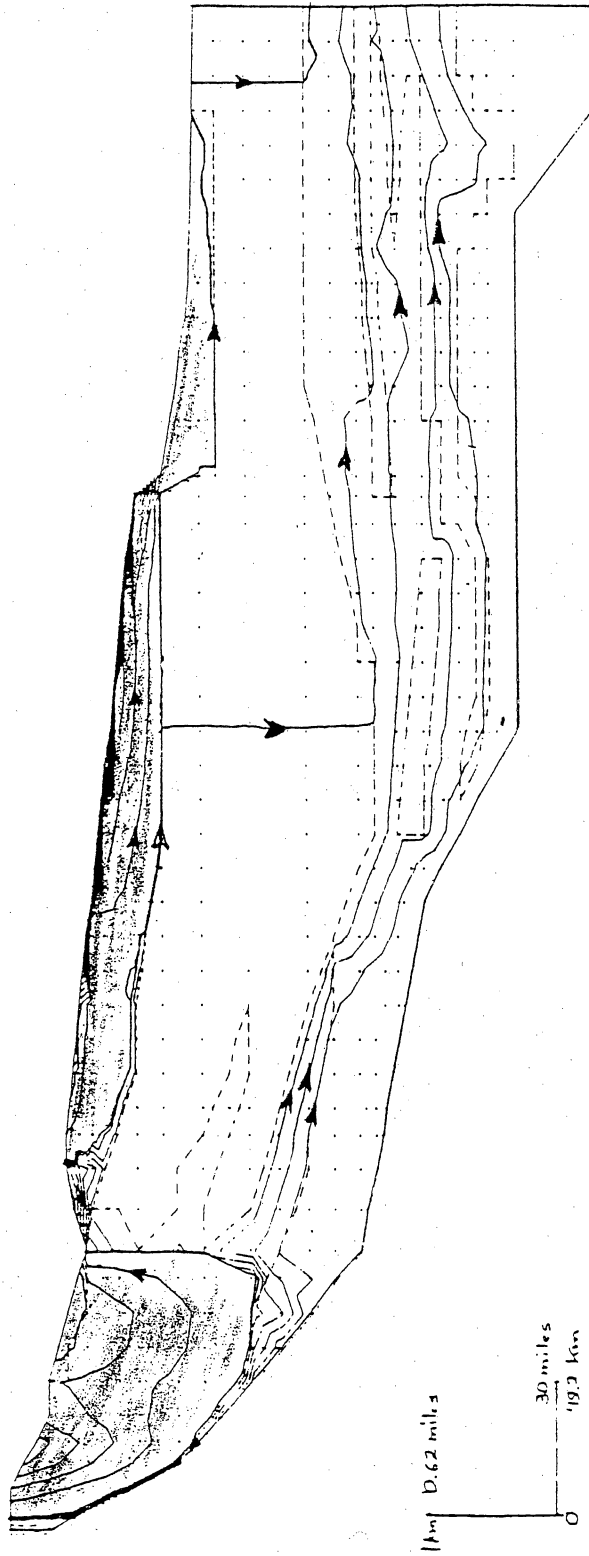


Figure 10. Isolith map of Pennsylvanian and Wolfcampian granite wash in the Texas Panhandle (after Dutton and others, 1982).

West  $N.H.K.$   $T_x$   $T_x$   $O.K.H.$  East






-  flow volume between two streamlines:  $0.01\text{m}^3/\text{day}$
-  flow volume between two streamlines:  $0.2\text{m}^3/\text{day}$
-  flow direction

Figure 11. Streamline distribution according to Simulation A-2. Ground-water flow is concentrated in the shallow aquifer system. Only a small fraction of flow is passing through the Deep-Basin Brine Aquifer.

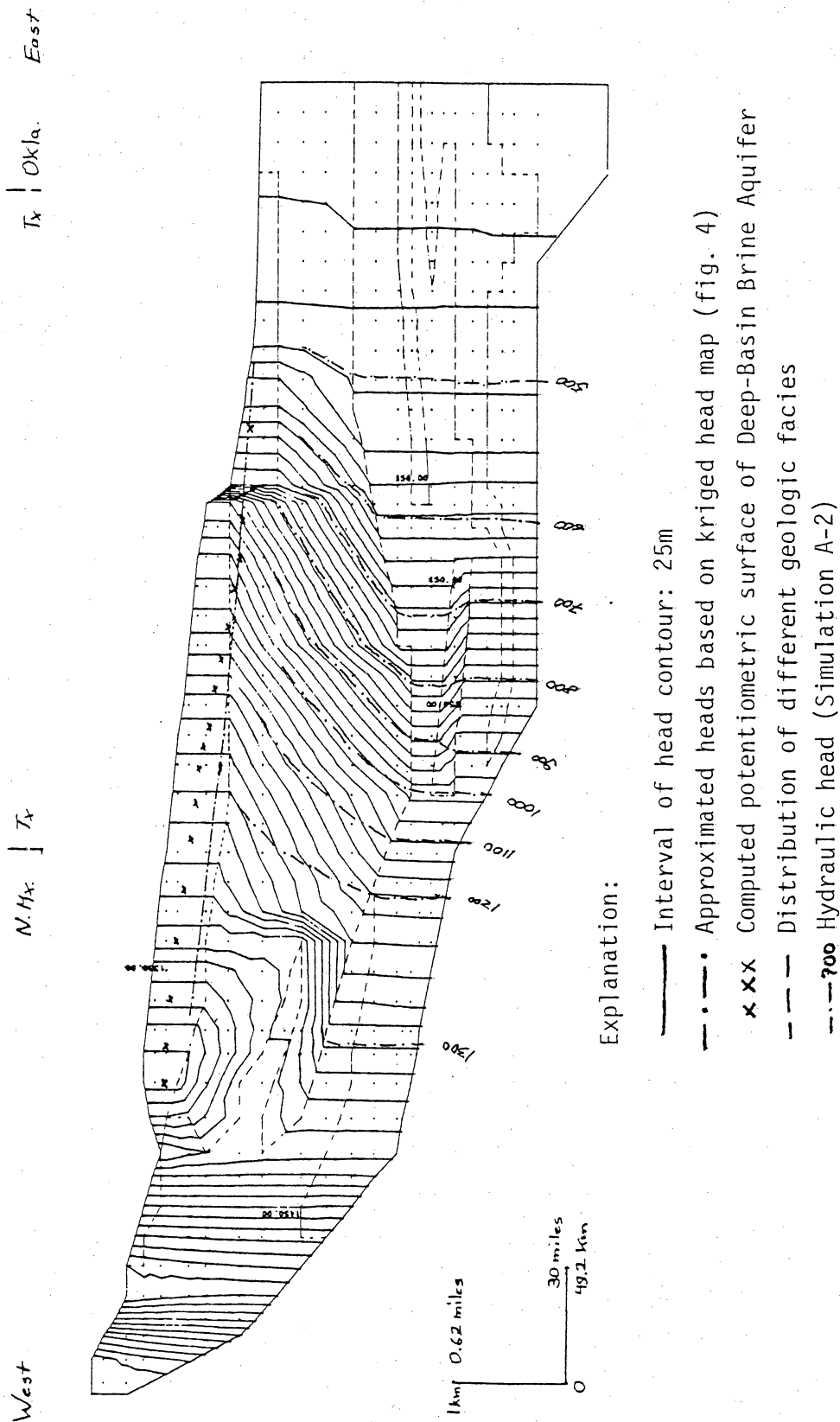


Figure 12. Simulation A-3 of computed hydraulic head distribution with increased hydraulic conductivities for granite wash as compared to Simulation A-2. It shows increased depressing toward the western part of the Deep-Basin Brine Aquifer.



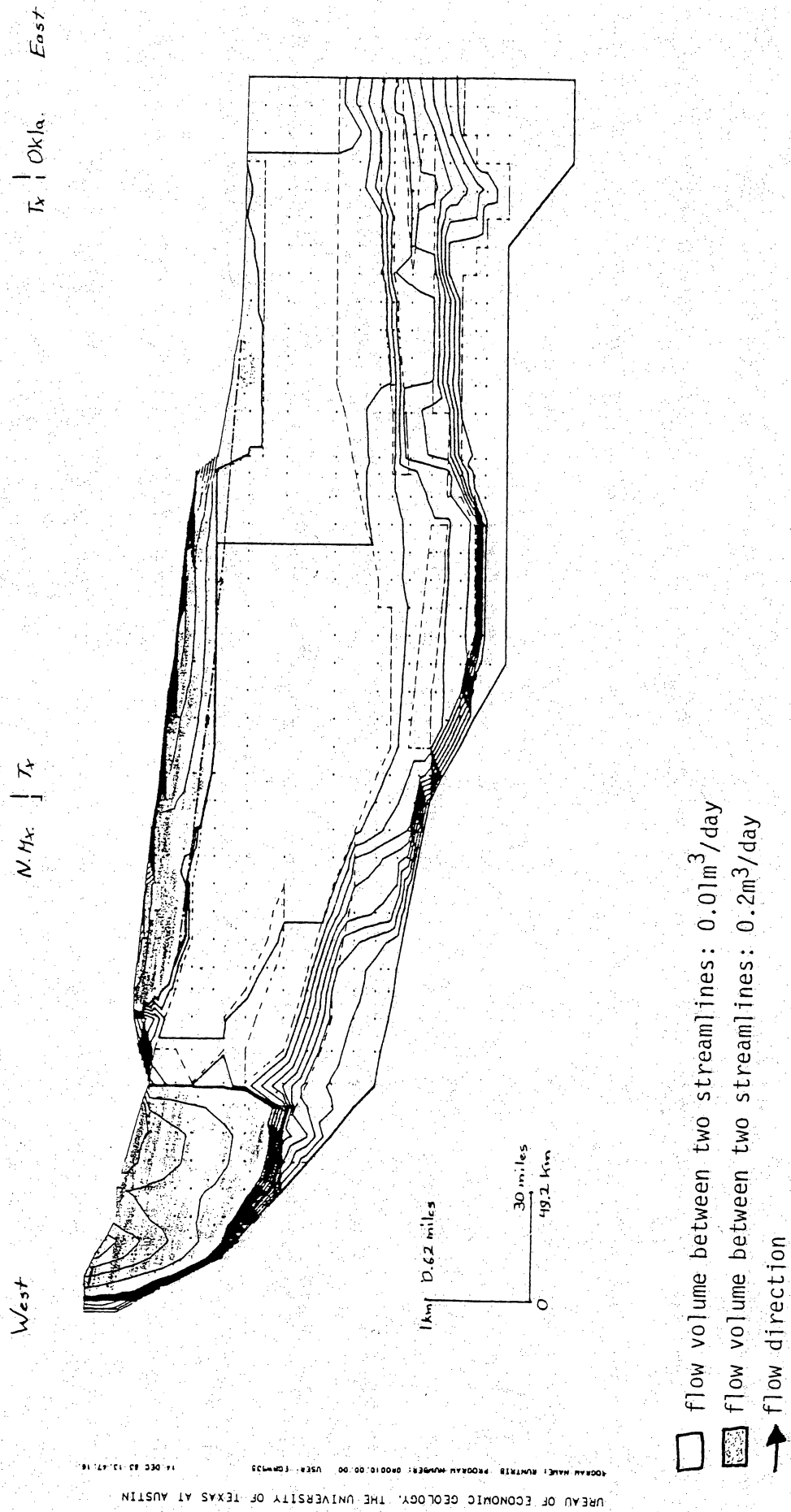


Figure 13. Streamline distribution according to Simulation A-3. Ground-water flow pattern within the Deep-Basin Brine Aquifer is governed primarily by the spatial distribution of relatively permeable granite-wash deposits.



Figure 14. Simulation B-1 of computed hydraulic head distribution with increased vertical permeability of the Evaporite Aquard. It shows a drastic head increase in the deep section.

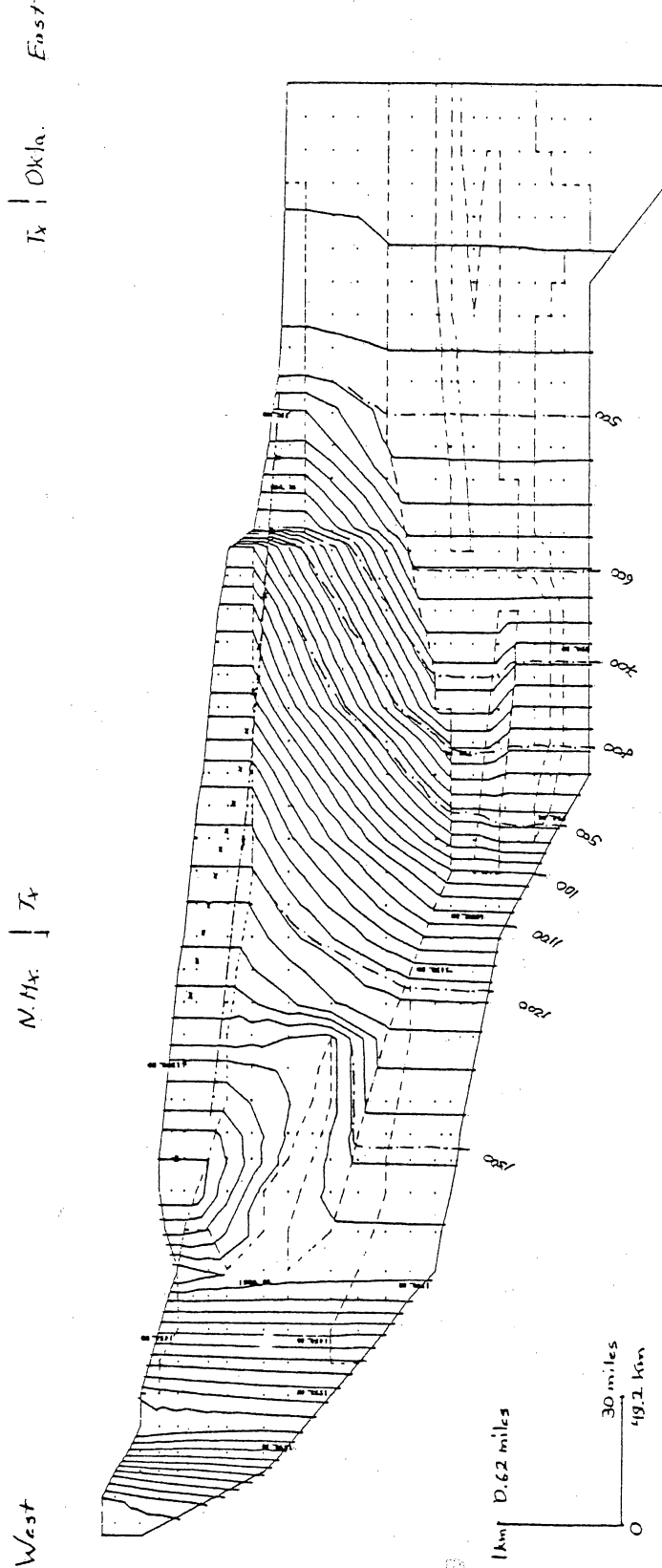
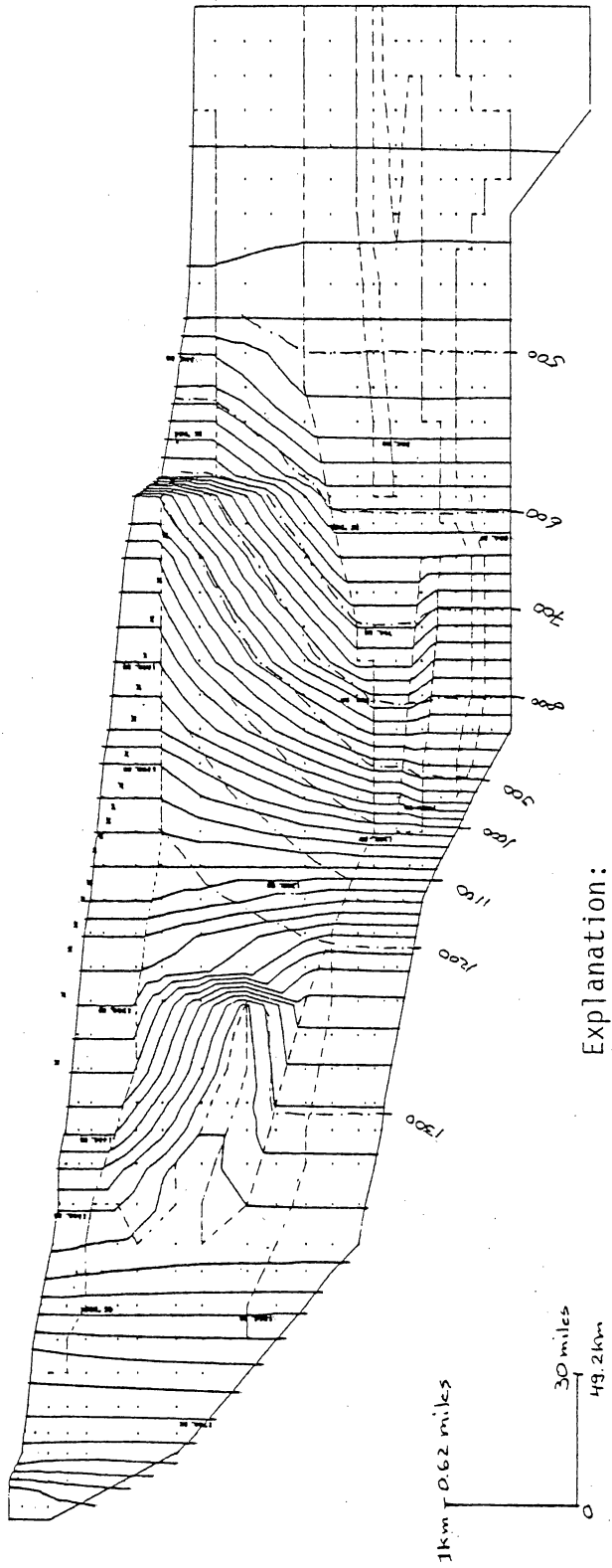


Figure 15. Simulation B-2 of computed hydraulic head distribution with decreased vertical permeability of the Evaporite Aquitard. It shows a general decrease of heads in the Deep-Basin Brine Aquifer by up to 50 m (164 ft) in the central part of the cross section.

West | Tx. | Okla. | East

West | Tx. | East

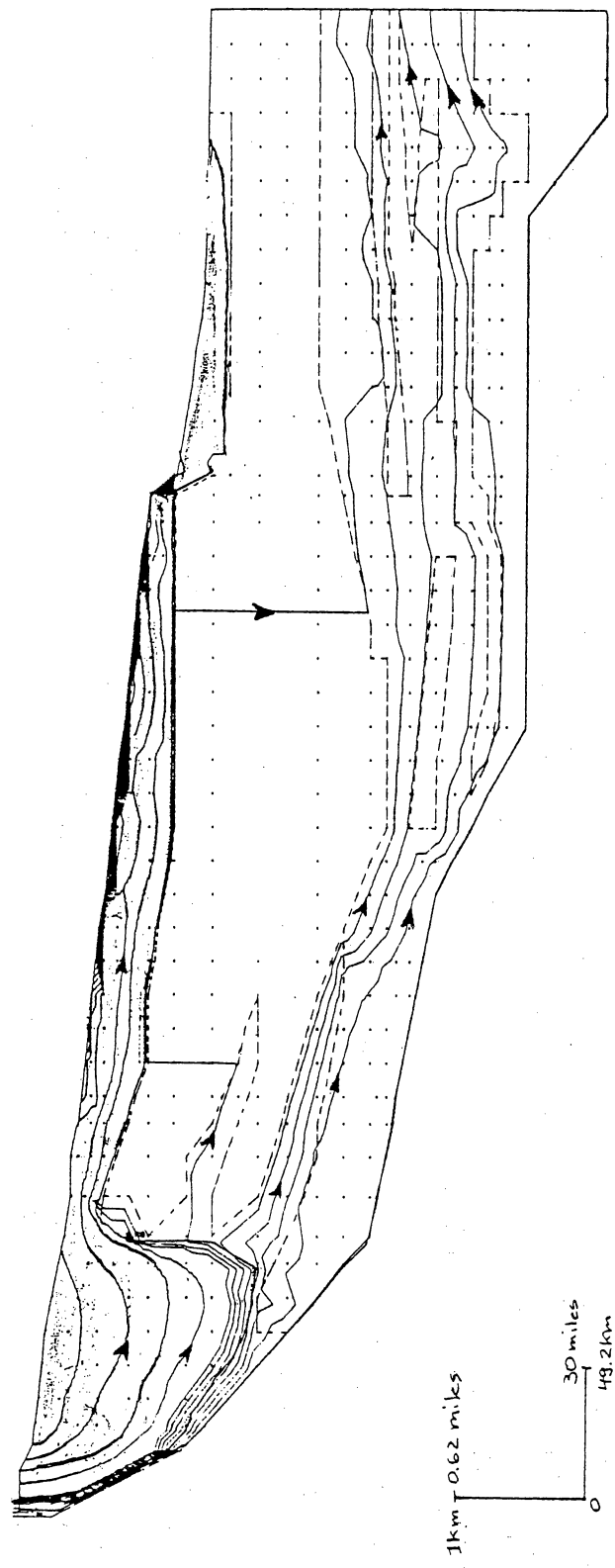


Explanation:

- Interval of head contour: 25m
- - - - - Approximated heads based on kriged head map (fig. 4)
- x x x Computed potentiometric surface of Deep-Basin Brine Aquifer
- - - Distribution of different geologic facies
- - - 700 Hydraulic head (Simulation A-2)

Figure 16. Simulation C of computed hydraulic head distribution with modified finite element mesh. It shows increased heads in the western part of the cross section. In the eastern part, however, extensive subhydrostatic conditions are maintained.

West  
N. Mex. | Tex. | Okla. East



- flow volume between two streamlines:  $0.01 \text{ m}^3/\text{day}$
- ▒ flow volume between two streamlines:  $0.2 \text{ m}^3/\text{day}$
- flow direction

Figure 17. Streamline distribution according to Simulation C. Ground-water flow into the Deep-Basin Brine Aquifer increased from 0.0034 (Simulation A-2) to  $0.047 \text{ m}^3/\text{day}$ .

West N. Hx. | T<sub>x</sub> T<sub>x</sub> | Okla. East

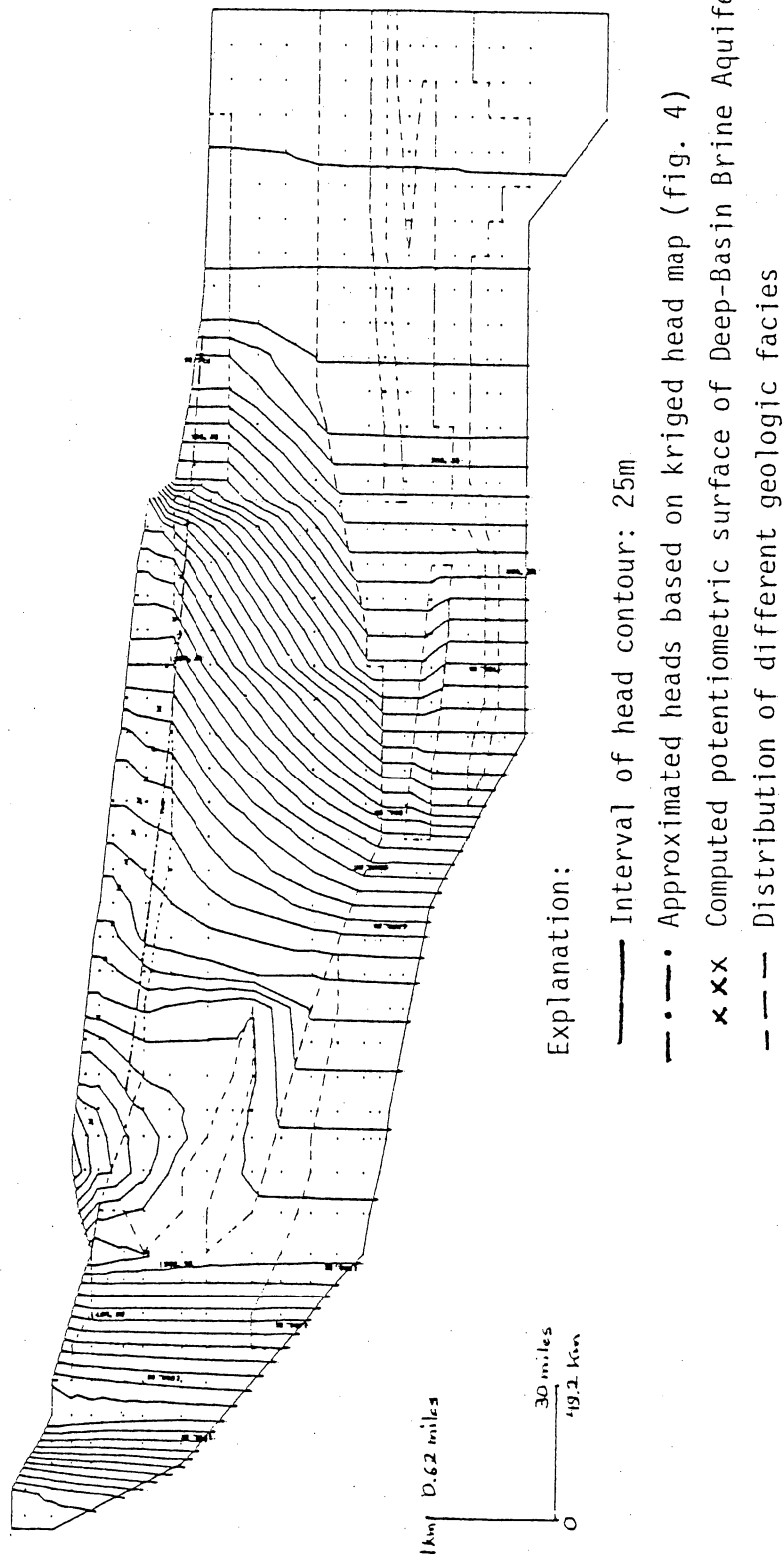


Figure 18. Simulation D of computed hydraulic head distribution considering vertical head differential within the shallow aquifer system. Hydraulic heads in the deep section are not significantly changed compared to heads in Simulation A-2.

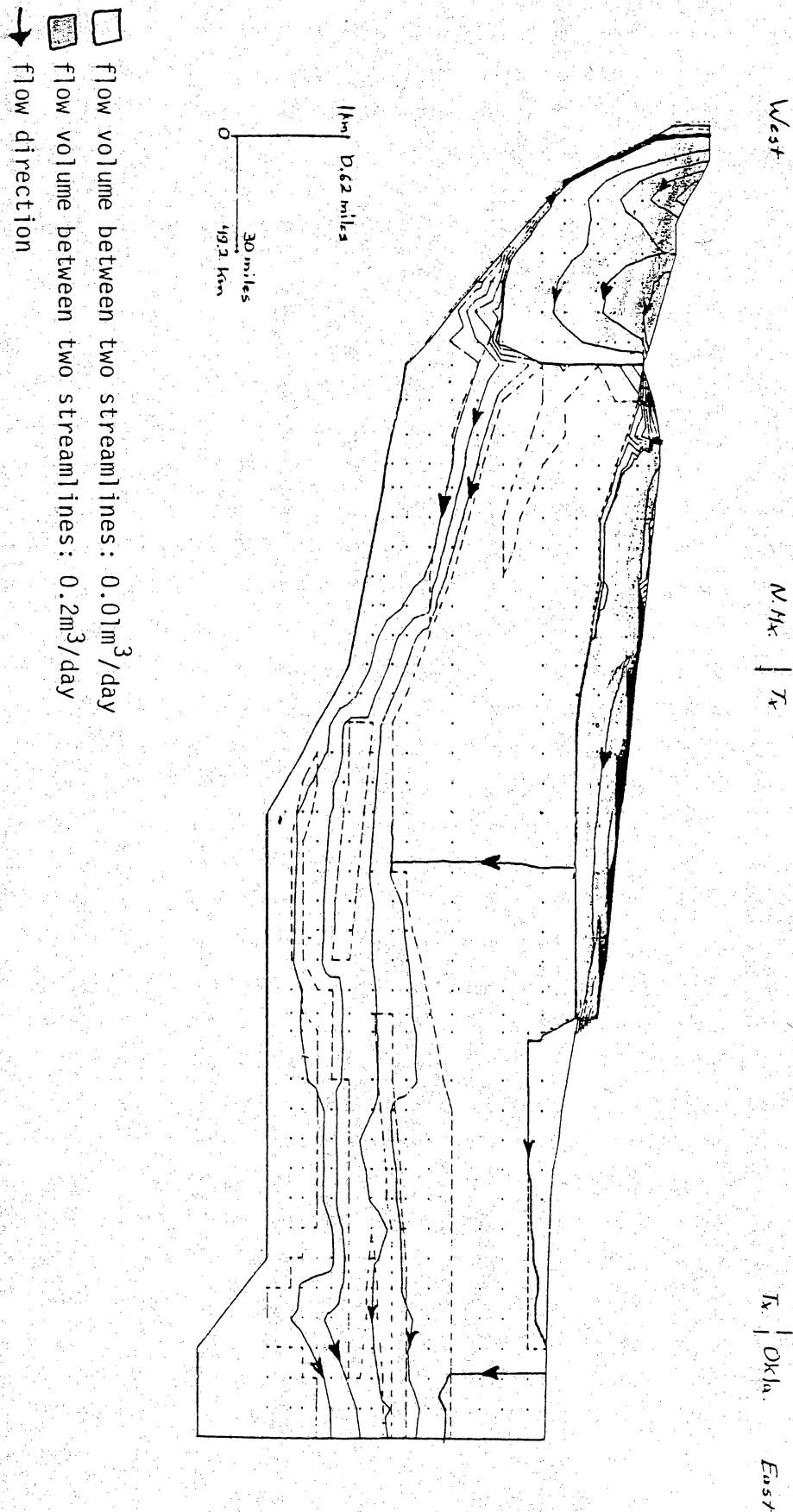


Figure 19. Streamline distribution according to Simulation D. The general ground-water flow pattern appears not to be affected by the vertical head differential in the Dockum. Vertical leakage through the Evaporite Aquitard, however, is reduced by about 19 %, as compared to Simulation A-2.